



Hybrid Nanoparticles for Detection and Treatment of Cancer

Michael J. Sailor* and Ji-Ho Park*

There is currently considerable effort to incorporate both diagnostic and therapeutic functions into a single nanoscale system for the more effective treatment of cancer. Nanoparticles have great potential to achieve such dual functions, particularly if more than one type of nanostructure can be incorporated in a nanoassembly, referred to in this review as a hybrid nanoparticle. Here we review recent developments in the synthesis and evaluation of such hybrid nanoparticles based on two design strategies (barge vs. tanker), in which liposomal, micellar, porous silica, polymeric, viral, noble metal, and nanotube systems are incorporated either within (barge) or at the surface of (tanker) a nanoparticle. We highlight the design factors that should be considered to obtain effective nanodevices for cancer detection and treatment.

1. Introduction and Motivations

In Isaac Asimov's 1966 novel Fantastic Voyage, scientists develop a technology that shrinks a team of people in a submarine to the size of a human blood cell.[1] The microscopic submarine is injected into the body of a comatose patient, and the passengers steer their craft through the body to find and remove a life-threatening blood clot. Modern-day scientists working in the field of nanotechnology often use this literary image to describe their vision. Though nanotechnologists aren't able to shrink people to those sizes, they are building the submarines, at least in the form of small devices that can circulate through the body, and they are imparting in those structures the capabilities to perform autonomous tasks to diagnose and treat patients. Like Asimov's microscopic submarine, the nanostructures we build today must possess many functions to be effective, and this has naturally led to the combining of multiple nano-objects into hierarchical assemblies. This

Prof. J.-H. Park Department of Bio and Brain Engineering Korea Advanced Institute of Science and Technology 291 Daehak-ro, Yuseong-gu, Daejeon 305-701, Korea E-mail: jihopark@kaist.ac.kr

Prof. M. J. Sailor Materials Science and Engineering Program Department of Chemistry and Biochemistry University of California San Diego, 9500 Gilman, La Jolla, CA 92093, USA

E-mail: msailor@ucsd.edu

DOI: 10.1002/adma.201200653



review focuses on what we call hybrid nanoparticles—nanoparticles that contain two or more distinct nanoparticles assembled in a functional structure that itself is still of nanoscale dimensions. The goal of this type of research is to build a nanostructure whose medical effects are superior to those that could be realized from any simple mixture of the individual components.

1.1. Nanoparticles to Detect and Treat Cancer

Nowhere in medicine are the goals of nanotechnology more hotly pursued than

in the field of oncology.[2-4] Researchers have created many examples of nanoparticles that can circulate through the bloodstream and stick to tumors. The optical or magnetic properties of some of these nanoparticles provide a means to image tumors at their earliest stages of development. For example, the strong superparamagnetism of magnetic nanoparticles allows the visualization of target diseased tissue in any plane of the body using T₂-weighted magnetic resonance imaging. [5-7] Additionally, the quantum confinement effect exhibited by semiconductor nanoparticles allows ultrasensitive and multiplexed fluorescence imaging both in vitro and in vivo, providing new tools to understand cellular processes related to cancer development.^[8,9] Other nanosystems can carry small payloads of anti-cancer drugs and deliver them directly to a tumor. For example, the high loading capacity and the biologically stable nature of lipid bilayer-based liposomes allow the delivery of drugs to target sites in vivo, minimizing side effects and toxicity of the drug payloads. [10,11] As a completely inorganic alternative, mesoporous silica nanoparticles have been used to secure and carry therapeutic agents in biological systems.^[12,13] Therapeutic functions other than drug delivery can be performed by nanoparticles engineered with the ability to transduce optical or radio frequency energy into thermal energy. The coupling of the strong near-infrared (NIR) plasmon resonance absorption of gold nanoparticles into thermal energy is an example of a nanoscale phenomenon that has been exploited to photothermally destroy malignant tumors.[14,15] Although such nanoscale characteristics can enhance the detection or treatment of cancer, the single functionality in all the above examples of nanosystems limits their utility, because multiple systems are required to detect, monitor, and treat cancer.

Makrials Views

www.MaterialsViews.com

1.2. Combining Multiple Functions into a Single Nanosystem: Hybrid Nanoparticles

Several oncology-directed nanosystems that integrate multiple nanocomponents and nanostructures into a single nanodevice have emerged. [16,17] Imaging of tumors provides a good example of where the properties of two nanodevices could be combined to improve surgical treatment of cancer patients. Whereas superparamagnetic iron oxide nanoparticles improve the contrast of magnetic resnonance images (MRI), the fluorescence of nanoparticle quantum dots can be seen by the unaided eye. A tumor-targeting nanosystem that possesses both types of nanoparticles offers the possibility to first identify a malignant tissue non-invasively by MRI, providing a low-resolution anatomical reference to guide the surgical procedure. Then, during surgery, the tumor margins can be directly visualized at a higher resolution by fluorescence imaging of the quantum dots. In addition, optical fluorescent systems can provide detailed subcellular information, which can aid in the diagnostic procedure.

Multiple nanocomponents with diagnostic and therapeutic functions can be integrated into a single nanosystem. [18–20] These systems follow on the concept of a "theranostic" device, in which both diagnostic and therapeutic functions can be administered in a single dose. [21] For nanoparticles, one advantage of combining imaging with therapeutic functions is that the biodistribution of the materials can be monitored *in vivo*, reducing the potential for unintended side effects of drug toxicity or hyperthermia-induced damage in healthy tissues. In addition to the utility of tracking the fate of nanotherapeutics *in vivo* immediately after administration, the use of such hybrid nanoparticles potentially allows the medical team to monitor the progress and efficacy of a therapy throughout the course of treatment.

1.3. General Design Rules for Hybrid Nanoparticles: Barges vs Tankers

In general there are two approaches to incorporate a therapeutic or diagnostic entity in a nanoparticle: it is either stuck to the surface of a solid nanoparticle, or it is encapsulated in a porous nanostructure. In a sense, this is related to the two methods of carrying goods on ships in the macroscopic world: we either stack the cargo on the deck of a barge or we place it in the closed container of a tanker. As with shipping, the solution chosen to carry a nano-cargo depends on the characteristics of the cargo and the delivery requirements. A reactive or antigenic drug should be protected from the environment in some sort of container vessel until it reaches its "port," whereas an imaging agent attached to the external surface of a barge-like vessel can be more readily accessed and more rapidly released in response to physiological stimuli.

One concept that does not translate well to the macroscopic shipping analogy is carrying capacity. For a macroscopic sphere, many more molecules can be contained in the inner volume than can be adsorbed on the surface. As the sphere gets smaller, the space available to load a drug either on the surface or in the interior volume decreases. However, as the diameter of the sphere approaches the dimensions of the molecular



Michael J. Sailor is the Leslie Orgel Scholar and Professor of Chemistry and Biochemistry at the University of California, San Diego. He holds Affiliate appointments in the Department of Bioengineering and in the Department of Nanoengineering. He received a B.S. degree in Chemistry from Harvey Mudd College, and M.S.

and Ph.D. degrees in Chemistry from Northwestern University. Following post-doctoral studies at Stanford and the California Institute of Technology, he joined the faculty in the Department of Chemistry and Biochemistry at the University of California, San Diego in 1990. He was promoted to Associate Professor in 1994, and to Full Professor in 1996. He is on the executive steering committee of the UCSD Materials Science Ph. D. program and a member of the Moores Cancer Center at UCSD.



Ji-Ho Park is an Ewon
Assistant Professor of Bio and
Brain Engineering at Korea
Advanced Institute of Science
and Technology (KAIST). He
received his B.S. degree in
Metallurgical Engineering
and his M.S. degree in
Medical Sciences from Yonsei
University (Seoul, Korea).
He received his Ph.D. degree
in Materials Science from

the University of California, San Diego (La Jolla, USA). His Ph.D. thesis work involved the engineering of biosafe nanomaterials and cooperative nanosystems for cancer diagnosis and therapeutics in the laboratory of professor Michael J. Sailor. He performed post-doctoral studies at University of California, Berkeley, working on nanowire-based systems for biological and energy applications under Peidong Yang. He joined the faculty in the Department of Bio and Brain Engineering at KAIST in 2010.

payload, more molecules can be placed on the surface than can be contained in the inner volume. A simple set of bounding calculations can be performed to answer the question "at what nanoparticle diameter is it more efficient to load a drug on the surface of a solid nanoparticle than in the interior of a hollow one?" The result depends on the size of the drug in question, and **Figure 1** presents the results for two different anti-cancer therapeutics, representing a small molecule (doxorubicin) and a large protein (the antibody drug bevacizumab, trade name

ADVANCED MATERIALS

www.advmat.de

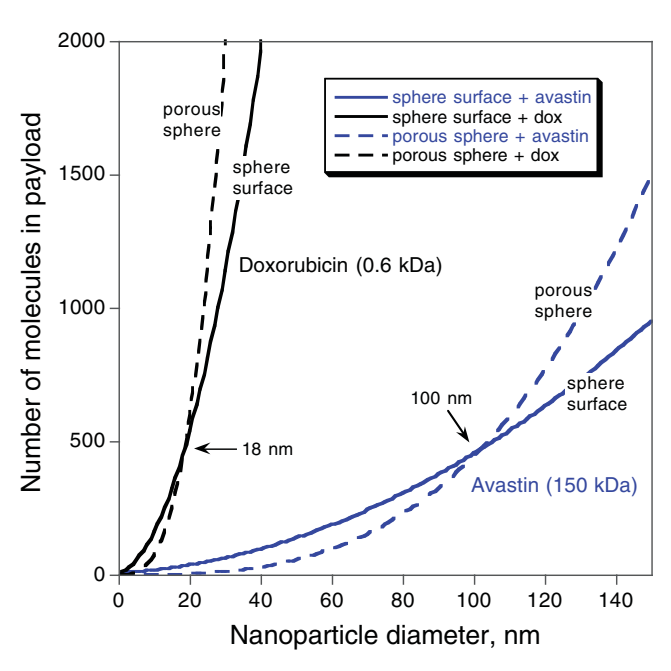


Figure 1. Calculation comparing the payload capacity of solid versus porous nanoparticles. The number of molecules in the payload that could be loaded on the surface of a solid nanoparticle ("sphere surface", solid lines) is compared to the number that could be contained within the confines of a hollow nanoparticle ("porous sphere", dashed lines), as a function of nanoparticle diameter. The result depends on the size of the drug payload, and the calculation is performed using two different anticancer drugs, the small molecule doxorubicin ("dox", black traces) and the large protein antibody bevacizumab, trade name Avastin ("avastin", blue traces). For these calculations, the hollow particles were loaded only in the interior (no molecules on the surface), while the solid particles were loaded only on the surface. In both cases the maximum loading is assumed to be hexagonal close packed (hcp), 74% packing efficiency, with the drug molecules approximated as spheres. In addition, the available volume in the porous nanoparticles is assumed to be 80% of the geometric volume.

Avastin). The plots in Figure 1 give the number of molecules that can be loaded as a function of nanoparticle diameter. As can be seen in the plots, the crossing point occurs when the nanoparticle carrier is ~ten times the diameter of the molecule payload: for the small molecule this occurs at ~20 nm, whereas for the large protein it is ~100 nm. At diameters less than these cutoffs, the nanoparticle can carry more molecules on its surface than in its inner volume. This "ten-fold" rule for host diameter vs payload diameter is very dependent on loading efficiency, which is usually much smaller in practice than in concept, but it provides a limiting guide for the design of a nanocarrier. As already mentioned, there may be biocompatibility issues that push one to choose an enclosed "tanker"-like nanostructure, but from the perspective of maximizing the quantity of drug delivered to a target tissue, it doesn't make sense to build a hollow nano-carrier at a size much smaller than 100 nm. A main advantage of the hollow "tanker" approach is that, in general, the loaded drug does not have to be chemically modified to load it into the nanocarrier as is required for surface-loaded "barge"-like nanocarriers. This can become a critical issue for regulatory approval—a chemically modified drug usually must

be treated as a new chemical entity, which can slow the path to the clinic significantly.

1.4. Biocompatibility Considerations

Probably the most important factor in the design of any nanoparticle for in-vivo application is the biocompatibility of the device. The term "biocompatibility" has many meanings. In some cases the mere demonstration of water solubility is cited as evidence of biocompatibility. In the present context, "biocompatible" means that the nanoparticle must display limited toxicity to the organism at its effective dose, it must be able to perform its function without interference from the organism's healthy mechanisms, and it must be able to circulate sufficiently long to accomplish its intended task. Shape, size, and charge are all factors in determining how long a given nano-particle will circulate before being eliminated by the liver, kidneys, or spleen. A key requirement for intravenously administered nanotherapeutics is that they have an ability to circulate in the bloodstream for >2 hours; if it is filtered out by the liver or the kidneys it can't make it to the tumor.

1.5. Specific Targeting to Tumors

The blood vessels feeding tumors tend to be very "leaky" relative to normal blood vessels. Many kinds of nanoparticles will find their way from the bloodstream into tumors via these leaky vessels. The phenomenon is known as EPR, for "Enhanced Permeability and Retention." Not everything in the blood stream will invade a tumor by this route, but on the whole it is a fairly non-specific mechanism that works for a wide range of nanoparticles. A more specific method to target a tumor is to attach molecules to the surface of the nanoparticle that have an affinity for tumor tissues or that can induce transport into cancerous cells. These molecules can be sugars, small molecules, antibodies, or small peptides; folic acid is one of the most commonly employed small molecules, which targets the folate receptor present on the surface of many tumor cells. [22,23]

2. Classification of Hybrid Nanoparticles

In this article, we focus on hybrid nanoparticles that contain both structural (therapeutic) and functional (diagnostic) nanocomponents (Table 1). As discussed in section 1.3, the functional nanocomponents such as gold nanostructures (for optical imaging), magnetic nanocrystals (for improving MRI contrast or hyperthermia), or quantum dots (for fluorescence imaging) can be either incorporated into the inner space of a structural nanocomponent ("tanker") or equipped on the surface of structural nanocomponent ("barge"). The structural components of the hybrid nanoparticles are mainly classified based on the therapeutic function they deliver. For example, structural nanocomponents such as a liposome, a micelle, mesoporous silica, a polymer, or a virus can mainly carry a drug cargo, while structural nanocomponents such as a gold nanoparticle or a carbon nanotube enable photoablation therapy (Table 2). The tumor



Table 1. Two principle design strategies for hybrid nanoparticles containing both therapeutic and diagnostic nanocomponents.

	Mo	ptif		
	Barge		Tanker	
Component	Nanoparticle t	ype	Function	Image key
Structural (therapeutic)	Liposome, micelle, porous s	Liposome, micelle, porous silica, polymer, and virus		
nanocomponent	Gold nanoparticle/nanoshell	/nanorod and	Photothermal	
-	carbon nanotube		heating	
Functional	Gold nanoparticle and quantum dot		Optical imaging	
(diagnostic)	Magnetic nanocrystal		MRI, magnetic	
nanocomponent			targeting	

targeting ability of these hybrid nanoparticles will be also discussed, as well as their diagnostic functions. Furthermore, we highlight important design factors to be considered for clinical translation. Hybrid nanoparticle systems that can be used for multimodal imaging are not included in this article, since several excellent reviews have recently appeared. [17,24,25] Hybrid nanoparticle systems incorporated with functional molecules (e.g., porphyrin, fluorophore, Gd molecule, radio-active molecule and so on) are not also included. A summary of the types

of hybrid nanoparticles that could be used for simultaneous diagnostics and therapeutics of cancer is presented in Table 3–9, categorized based on the type of structural nanocomponent.

2.1. Liposomal Hybrid Nanoparticles

Liposomes are "spherical", self-assembled nanostructures consisting of concentric lipid bilayers that can incorporate

Table 2. Intrinsic properties of structural nanocomponents in hybrid nanoparticles.

Structural nanocomponent	Intrinsic property					
	Therapeutic property	Diagnostic property	Biocompatibility			
Liposome	Loading of hydrophobic and hydrophilic drugs	N/A	Biodegradable			
Micelle	Loading of hydrophobic drugs	N/A	Biodegradable			
Mesoporous silica	Loading of hydrophilic drugs	N/A	Biodegradable			
Polymer (PLGA)	Loading of hydrophobic drugs	N/A	Biodegradable (in a controlled manner)			
Virus	Loading of therapeutic nucleic acids and efficient transfection	N/A	Biodegradable			
Gold nanoparticle	Photoablation therapy	Two-photon-induced photoluminescence (TPIP), surface enhanced Raman spectroscopy (SERS), computed tomography (CT), optical coherence tomography (OCT), and photoacoustic imaging,	Bioinert (non-biodegradable)			
Carbon nanotube	Photoablation therapy and loading of hydrophobic drugs	NIR fluorescence, Raman, optical coherence tomography (OCT), and photoacoustic imaging	Bioinert (non-biodegradable)			



Table 3. Representative liposomal hybrid nanoparticles for simultaneous imaging and therapy of cancer.

Structural nanocomponent	Functional nanocomponent		Target (tumor) cells or xenografts [targeting mechanism/	Ref.
Type (incorporated therapeutic payload and other function)	Type (diagnostic and other function)	Design	species employed]	
Phospholipid liposome (no payload and membrane fusion)	Gold nanoparticle (optical imaging)	Barge	Jurkat cells (T-lymphocyte, nonadherent) [membrane fusion]	[35]
Phospholipid liposome [calcein (model drug)]	Gold nanoparticle (photothermal heating-triggered drug release)		ARPE-19 human retinal pigment epithelia cells [non-specific internalization]	[34]
Phospholipid liposome [6-carboxyfluorescein (model drug)]	Gold nanoparticle (photothermal heating-triggered drug release)	Tanker	N/A	[28]
Phospholipid liposome [Xylenol orange sodium salt (model drug)]	Magnetic nanocrystal (MRI)	Barge	N/A	[42]
Phospholipid liposome [5,6-Carboxyfluorescein (model drug)]	Magnetic nanocrystal (electromagnetic heating-triggered drug release)		N/A	[43]
Phospholipid liposome (doxorubicin or cysteine protease inhibitor JPM-565)	Magnetic nanocrystal (MRI and magnetic targeting)	Tanker	MMTV-PyMT human breast cancer cells and xenografts [magnetic targeting]	[44]
Phospholipid liposome (N/A)	Quantum dot (optical imaging)	Barge	A549 human epithelial lung cells [non-specific internalization]	[31]
Phospholipid liposome (doxorubicin)			MCF-7/HER2 cells and xenografts [anti-HER2 single chain Fv fragments]	[59]
		Tanker	A431 human epithelial carcinoma cells [epidermal growth factor (EGF) ligand]	[51]

hydrophilic therapeutic agents in their internal spaces or hydrophobic drugs within the bilayers. Small unilamellar liposomes which have been widely used for cancer therapy have the size range of 50-150 nm and are nanoassemblies with a single bilayer.[11] In particular, liposomes constructed of lipids that contain a poly (ethylene glycol) (PEG) pendant strand have been found to be capable of circulating for relatively long periods of time before being eliminated. These long-circulating liposomes can passively accumulate in tumors through the porous endothelium present in tumors—the EPR effect described above. Drugs incorporated into the liposomes can be released slowly in tumors, generating high local concentrations of drug and minimizing the systemic dose. Once the drug is delivered, the dissociated lipids are harmlessly cleared from the body. These attractive features have led to broad interest in liposomal systems for delivery of various chemotherapeutic agents

Table 4. Representative micellar hybrid nanoparticles for simultaneous imaging and therapy of cancer.

Structural nanocomponent	Functional nanocomponent		Target (tumor) cells or xenografts [targeting	Ref.
Type (incorporated therapeutic payload and other function)	Type (diagnostic and other function)	Design	mechanism/species employed]	
PCL-b-PGMA micelle (paclitaxel)	Magnetic nanocrystal (MRI)	Barge	N/A	[91]
PEG-PLA micelle (doxorubicin)		Tanker	SLK tumor endothelial cells [$lpha_{v}eta_{3}$ -integrin targeting cRGD peptide]	[97]
PEG-PLA micelle (doxorubicin)			H2009 lung adenocarcinoma cells [lung cancer targeting peptide with a sequence of RGDLATLRQL]	[98]
Phospholipid micelle (siRNA)			MKN-74 and NUGC-4 gastric adenocarcinoma cells [anti-EGFR antibody]	[99]
HAMAFA-b-DBAM micelle (doxorubicin and pH-sensitivity)			KB human carcinoma cells [folic acid]	[101]
PEG-PAsp(DIP)-CA micelle (paclitaxel and pH-sensitivity)	Quantum dot (optical imaging)	Barge	Bel-7402 human hepatocellular carcinoma cells [folic acid]	[96]
PEG-phospholipid micelle (doxorubicin)	Magnetic nanocrystal (MRI) and quantum dot (optical imaging)	Tanker	MDA-MB-435 human breast cancer cells and xeno- grafts [F3 tumor targeting peptide for <i>in vitro</i> and passive targeting by EPR for <i>in vivo</i>]	[19]
PS-b-PAA micelle (doxorubicin)	Magnetic nanocrystal (MRI and magnetic targeting)	Tanker	4T1 murine breast cancer cells and xenografts [passive targeting by EPR]	[1,102]
	Upconversion nanoparticle (optical imaging)			

Adv. Mater. 2012, DOI: 10.1002/adma.201200653



 Table 5. Representative porous silica-based hybrid nanoparticles for simultaneous imaging and therapy of cancer.

Structural nanocomponent	Functional nanocomponent	Functional nanocomponent		Ref.
Type (incorporated therapeutic payload and other function)	Type (diagnostic and other function)		nism/species employed]	
Porous silica (doxorubicin)	Magnetic nanocrystal (MRI)	Barge	MCF7 human breast cancer cells [passive targeting by EPR]	[134]
Porous silica (camptothecin or paclitaxel)		Tanker	PANC-1 and BxPC3 human pancreatic cancer cells [folic acid]	[123]
Porous silica (doxorubicin)			H446 human lung cancer cells [folic acid]	[127]
Porous silica (photosensitizer ZnPc)	${\sf NaYF_4}$ up-conversion nanocrystal (optical imaging & excitation source for photosensitizer)		MB49 murine bladder cancer cells [non-specific endocytosis]	[133]
Porous silica (photosensitizer hematoporphyrin)	Gold nanorod (optical imaging and photothermal heating)		MDA-MB-231 human breast cancer cells (non-specific internalization)	[132]
Porous silica (both doxorubicin and cisplatin, and liposomal coating)	Quantum dot, loaded into the porous nanostructures (optical imaging)		Hep3B human hepatocellular carcinoma cells [HCC targeting SP94 peptide with a sequence of SFSIIHTPILPLGGC]	[137]
Porous silica nanorattle (docetaxel)	Gold nanoshell (optical imaging and photothermal heating)	Barge	HepG2 human hepatocellular carcinoma cells and H22 mouse hepatoma xexnografts [passive targeting by EPR]	[141]

 Table 6. Representative polymeric hybrid nanoparticles for simultaneous imaging and therapy of cancer.

Structural nanocomponent	Functional nanocomponer	nt	Target (tumor) cells or xenografts [targeting mechanism/ species employed]	Ref.
Type (incorporated therapeutic payload and other function)	Type (diagnostic and other function)	Design		
PLGA (doxorubicin and thermosensitive drug release)	Gold nanocoating (photothermal heating)	Barge	A431 human epidermoid carcinoma cells and xenografts [passive targeting by EPR]	[167]
PLGA (doxorubicin and controlled drug release)	Magnetic nanocrystal (MRI)	Tanker	NIH3T6.7 fibroblast cells [herceptin]	[172]
PLGA (doxorubicin and controlled drug release)	Magnetic nanocrystal (MRI)		KB human carcinoma cells [folic acid]	[162]
PLGA (coenzyme Q10 and controlled drug release)	Quantum dot (optical imaging)		PC12 pheochromocytoma cell [passive internalization]	[161]
Polystyrene and PLGA (paclitaxel and	Quantum dot (optical imaging)	Barge	LNCaP human prostate cancer cells [anti-prostate specific	[171]
controlled drug release)	Magnetic nanocrystal (MRI)	Tanker	membrane antigen]	
PLGA (paclitaxel and controlled drug	ed drug Gold nanorod (photothermal heating) Tanker A549 human lung cance		A549 human lung cancer cells and xenografts [anti-Her2	[168]
elease)	Magnetic nanocrystal (MRI)		antibody for in vitro and intratumoral injection for in vivo]	
	Quantum dot (optical imaging)			

 Table 7. Representative viral hybrid nanoparticles for simultaneous imaging and therapy of cancer.

Structural nanocomponent	Functional nanocomponent		Target (tumor) cells or xenografts [targeting mechanism/	Ref.
Type (incorporated therapeutic payload and other function)	Type (diagnostic and other function)	Design	species employed]	
Adenovirus (eGFP gene)	Magnetic nanocrystal (MRI)	Barge	U251N cells [Coxsackie B on adenovirus]	[199]
Adenovirus (luciferase reporter gene)	Gold nanoparticle (photothermal heating)		HeLa and MC38-CEA-2 cells [Coxsackie B on adenovirus, and adenovirus engineered to target tumor-associated carcino embryonic antigen (CEA), respectively]	[200]
Cowpea mosaic virus (N/A)	C ₆₀ carbon nanoparticle (photodynamic therapy)		N/A	[201]
M13 bacteriophage (N/A)	Carbon nanotube (optical imaging)		LNCaP human prostate adenocarcinoma cells [anti- prostate specific membrane antigen antibody]	[203]
Human immunodeficiency virus (N/A)	Gold nanoparticle (photothermal heterodyne imaging)	Tanker	N/A	[202]

Adv. Mater. 2012, DOI: 10.1002/adma.201200653

www.iviateriaisviews.com

Table 8. Representative gold-based hybrid nanoparticles for simultaneous imaging and therapy of cancer.

Structural nanocomponent	Functional nanocomponent		Target (tumor) cells or xenografts [targeting mechanism/	Ref.
Type (therapeutic and other function)	Type (diagnostic and other function)	Design	species employed]	
Gold nanorod (photothermal therapy and fluorescence imaging)	Magnetic nanocrystal (MRI)	Barge	SK-BR-3 breast cancer cells [Herceptin]	[236]
Gold nanoshell (photothermal therapy)	Magnetic nanocrystal (MRI)	Tanker	SKBR3 breast cancer cells [anti-HER2/neu]	[18]
Gold nanoshell (photothermal therapy)	Magnetic nanocrystal (MRI)		MDA-MB-468 cells [anti-epidermal growth factor receptor]	[234]
Gold nanoshell (photothermal therapy)	Magnetic nanocrystal (MRI and magnetic targeting)	Barge	KB human epidermoid carcinoma cells and xenografts [folic acid and magnetic targeting]	[241]
	Upconversion nanocrystal (optical imaging)	Tanker		

Table 9. Representative carbon nanotube-based hybrid nanoparticles for simultaneous imaging and therapy of cancer.

Structural nanocomponent	Functional nanocomponent		Target (tumor) cells or xenografts [targeting mechanism/ species employed]	Ref.
Type (therapeutic and other function)	Type (diagnostic and other function)	Design		
Multi-walled carbon nanotube (photothermal therapy)	Magnetic nanocrystal (MRI)	Tanker	Murine renal carcinoma cells [passive targeting by EPR]	[276]
Single-walled carbon nanotube (incorporation of therapeutic molecule cisplatin)	Quantum dot (optical imaging)	Barge	Head and neck squamous carcinoma cells and xenografts [anti-epidermal growth factor receptor (EGFR) antibody]	[278]
Multi-walled carbon nanotube (N/A)	Quantum dot (optical imaging)		N/A	[277]
Multi-walled carbon nanotube (incorporation of therapeutic molecule gemcitabine)	Magnetic nanocrystal (magnetic targeting)		BxPC-3 human pancreatic cancer cells and in vivo meta- static model (magnetic targeting)	[272]
Single-walled carbon nanotube (photothermal therapy)	Gold nanocrystal (SERS imaging and photothermal therapy)		SK-BR-3 human breast adenocarcinoma cells	[283]

in cancer therapy, and many translational studies have been performed, with more underway, to bring liposomes into the clinic.

The use of liposomes for *in vivo* imaging has a long history.^[10] Various reporter moieties can be either attached on the surface of liposomes or incorporated into their internal water reservoir, prolonging the blood residence time of such molecules. Early studies found that liposomes decorated with paramagnetic molecules enable the detection of angiogenesis *in vivo* by magnetic resonance imaging (MRI).^[26,27] It has been recognized that various types of inorganic nanoparticles offer similar or improved image contrast in either MRI or other types of medical imaging systems, and iron oxide-based magnetic nanoparticles (for MRI), gold nanoparticles and luminescent quantum dots (for optical imaging) have been incorporated into various hybrid liposome systems.

For optical imaging and photothermal heating, hydrophilic gold nanoparticles have been encapsulated in the interior [^{28]} or on the outer membrane of liposomes, [^{29–31]} and hydrophobic gold nanoparticles have been inserted into the hydrophobic interior of the liposomal membrane (Table 3). [^{32–34]} A variety of imaging modalities can be incorporated into a liposomal formulation using gold nanoparticles. Feldmann and co-workers demonstrated that liposomes linked with gold nanoparticles can fuse with the cellular membrane, and the strongly scattered

light from the gold nanoparticle allowed its dynamic motion to be imaged.^[35] Photothermal heating in these systems relies on the strong coupling of an optical field into the plasmonic band of the gold nanoparticle. This can trigger secondary processes, such as chemical dissolution, which can then result in release of therapeutic agents from various types of nanoparticles.[36-38] For example, Zasadzinski and co-workers demonstrated drug release from a gold nanoparticle/liposome construct triggered by application of NIR light.^[28] Hollow gold nanoshells (HGN), with a wavelength of maximum absorption (λ_{max}) at 820 nm were used, and the HGN were either encapsulated by the liposomes, tethered to the liposomes, or physically mixed with liposomes as separate entities. It was found that HGN tethered directly to the outer surface of liposomes displayed the largest release of the liposomal payload—up to 93%—relative to other hybrid formulations. Thus the efficiency of photo-triggered release is related to the proximity of the light-absorbing nanoparticle to the lipid bilayer of the liposome. In addition to the local thermal effect, mechanical disruption by nano- or microbubbles generated during irradiation could also be responsible for the transient membrane ruptures. Möhwald and co-workers fabricated a similar assembly composed of liposomes and gold nanoparticles and demonstrated NIR laser-initiated release from a liposome. [39] Aggregation of gold nanoparticles, driven by electrostatic interactions between liposomes, resulted in

- Malerials Views

www.MaterialsViews.com

a red-shift of the plasmonic absorption (from 520 nm for an individual nanoparticle to 650 nm for the aggregation). Focused laser illumination of the assembly, loaded with a model drug (fluorescent dye), initiated rapid release of the encapsulated dye molecules. Combined therapy with anti-cancer drugs and photothermal heating could also be achieved with such a nanogold-incorporated liposomal formulation.

For MR imaging and electromagnetic heating, hydrophilic magnetic nanocrystals have been either encapsulated in the inner aqueous compartment^[40,41] or coated on the surface of liposomal nanovehicles, [42] and hydrophobic magnetic nanocrystals have been inserted into the hydrophobic interior of the liposomal membrane (Table 3).[43] Particularly, clustering of magnetic nanocrystals inside the liposome significantly improved their MRI contrast properties. [44,45] Kobayashi and coworkers developed magnetite-containing cationic liposomes for an intracellular hyperthermia application. [46,47] These magnetic liposomes were used as mediators to couple and convert irradiation from an alternating magnetic field operating at radio frequencies to generate localized heating. This electromagnetic heating of magnetoliposomes was utilized to release encapsulated therapeutic molecules to the surrounding environment, caused by the combined effects of bilayer permeabilization and partial membrane rupture. [43] Thermosensitive liposomes could further improve thermally controlled release of the encapsulated drugs.^[48] Highly concentrated magnetic nanocrystals inside the liposome were able to generate a therapeutically effective dose of thermal energy to malignant tissues within a clinically acceptable irradiation range. Furthermore, magnetic liposomes have been steered to tumors in vivo using an external magnet, and the distribution of the nanodevices has been identified by MR imaging.^[49]

For optical imaging, hydrophilic quantum dots have been encapsulated in the interior[50-52]or on the outer membrane of liposomes,[51,53] and hydrophobic quantum dots have been inserted into the hydrophobic interior of the liposomal membrane (Table 3).[31,50,54] Vogel and co-workers have incorporated hydrophobic quantum dots into the bilayer membrane of lipid vesicles.^[55] Interestingly, the selectivity of interaction of cationic hybrid liposomal nanoparticles with cells has been found to be dependent on the presence of PEG groups in the lipid layer. For example, hydrophobic quantum dots are dissociated from a PEGylated liposome and delivered to a cell's plasma membrane. whereas a non-PEGylated liposome containing the same type of quantum dots will become internalized into the cells in its entirety. Kostarelos and co-workers synthesized quantum dotliposome nanohybrids by encapsulating hydrophilic quantum dots into the aqueous core of a PEGylated cationic liposome.^[56] The PEGylated cationic fluorescent liposomes circulated for a relatively long time in the bloodstream of mice after systemic administration, ultimately accumulating in the tumor. These fluorescent nanohybrids then remained in the tumor for at least 24 hours, offering a wide temporal window for tumor imaging. Ménager and co-workers prepared liposomal hybrid vesicles with dual-imaging capabilities using an emulsion process to encapsulate two types of nanoparticles.^[57] The hybrid vesicles contained both hydrophilic magnetic nanoparticles and hydrophobic quantum dots, and displayed strong magnetic properties with little deleterious photobleaching. After intravenous injection in a mouse, the intense fluorescence of the hybrid vesicles allowed clear detection in several organs. Although these hybrid vesicles demonstrated the feasibility of such systems for $in\ vivo$ applications, they were not optimal formulations due to their large size (0.5 \sim 1 μ m) and short $in\ vivo$ circulation times.

A few reports have appeared describing the use of such hybrid liposomal nanoparticles for simultaneous targeting, diagnosis, and chemotherapeutic treatment of cancer (Table 3).[42,54] Nobuto and co-workers examined the efficiency of systemic chemotherapy administered using liposomes containing both magnetic nanocrystals and doxorubicin (DOX) in an osteosarcoma-bearing hamster.^[58] After intravenous administration of the magnetic DOX liposomes, a DC dipole electromagnet was turned on in the vicinity of the tumor. Greater accumulation of DOX in the tumor and significant improvement in the anti-tumor effect of the drug were observed. Although the targeting in this case was a bit crude, relying on the preexisting knowledge of the tumor location, it demonstrates the important advantage of multi-modal nanosystems. Park and co-workers developed a similar liposomal system, but using a specific antibody to provide molecular targeting, (Figure 2).^[59] An Anti-HER2 antibody and luminescent quantum dots were chemically linked to functional PEG groups on the liposome surface, and the interior of the liposomes contained a DOX payload. The researchers were able to verify localization at tumor sites both in vitro and in vivo by observation of luminescence from the quantum dots. This study demonstrated the feasibility of real-time observation of the dynamics of drug delivery to a targeted tumor site. Recently, Vasiljeva and co-workers used magnetic liposomes to localize therapeutic molecules in both the tumor and its microenvironment while monitoring their delivery by MRI.[44] In an orthotopic murine mammary tumor model, these MRI-visible liposomes delivered cysteine cathepsin inhibitors effectively to a tumor under the influence of an external magnet, substantially suppressing tumor growth.

Hybrid liposomal nanosystems have great potential for future clinical use since they are designed to integrate the well-established physicochemical and pharmacodynamic properties of liposomes with unique photochemical and electromagnetic properties of nanocrystals. However, careful attention should be paid to stability of such malleable systems since co-encapsulation of nanocrystals and therapeutics into the inner space of a liposome, insertion of nanocrystals into the liposomal membrane, or chemical attachment of nanocrystals to its surface all have the potential to cause payload leakage or a decrease *in vivo* stability of the liposomal nanostructure.

2.2. Micellar Hybrid Nanoparticles

Although liposomes can incorporate poorly soluble therapeutics in the thin hydrophobic bilayer that comprises the outer skin of these nanostructures, the drug loading capacity is somewhat restricted because of possible membrane destabilization and the relatively limited space available. Micelles are colloidal nanoparticles with smaller sizes (5–50 nm) compared to liposomes (50–150 nm). However, their inner volume is composed of hydrophobic tails of the lipid or surfactant constituents, into which many hydrophobic or amphiphilic molecules can

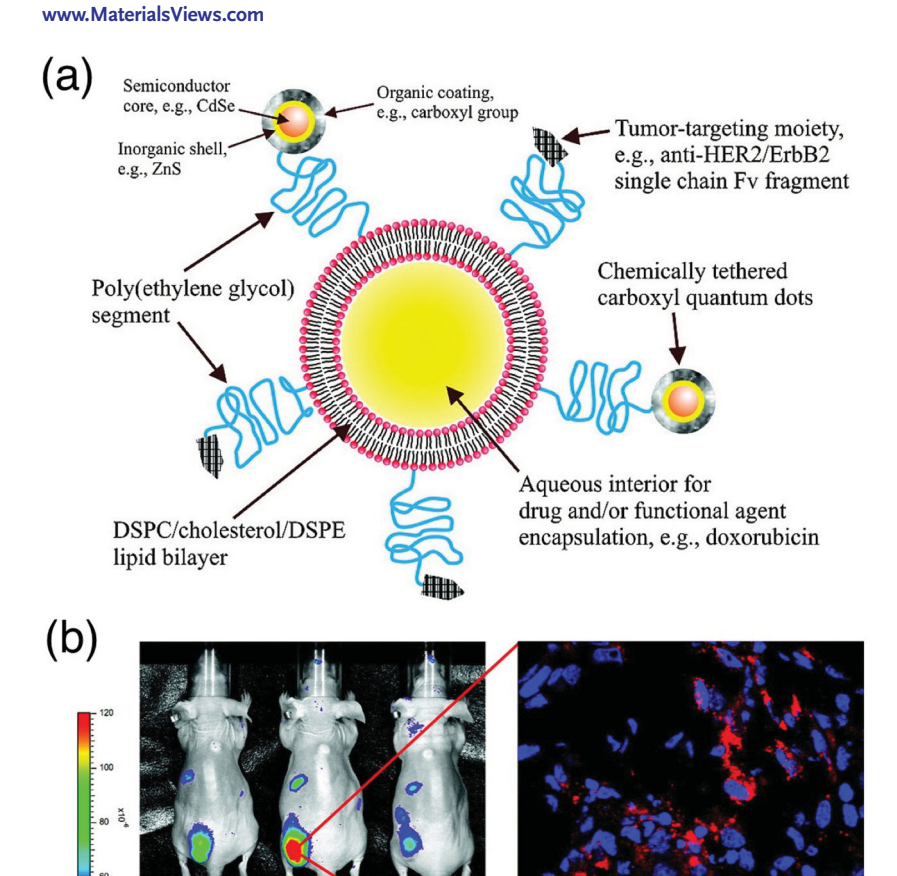


Figure 2. a) Schematic showing a liposomal hybrid nanoparticle containing antibody and quantum dot functionalities (QD-immunoliposomes). The pendant antibody provides a targeting capability, while the quantum dot exhibits bright photoluminescence to enable *in vivo* or *in vitro* imaging. b) (Left panel) *In vivo* fluorescence images of mice bearing MCF-7/HER2 xenograft tumors implanted in the lower back, 30 h after intravenous injection with QD-immunoliposomes. Fluorescence intensity is displayed in false color; the high intensity at the tumor site demonstrates that the liposomes accumulate prominently in tumors. (Right panel) Confocal fluorescence image of a tumor slice from the mouse, 48 h post-injection. Red and blue indicate QD-immunoliposomes and cell nuclei (DAPI stain), respectively. The QD-immunoliposomes appear to internalize into the cytosol of MCF-7/HER2 tumor cells *in vivo*. Reproduced with permission from ref. [59] Copyright © 2008 American Chemical Society.

self-assemble.^[60–62] In an aqueous environment, hydrophobic regions of amphiphilic molecules segregate to the core of the micelle and the hydrophilic regions of the molecules tend to orient into the aqueous phase, increasing the stability of the colloidal assembly. The hydrophobic core of a micelle is thus ideally suited for many types of hydrophobic or poorly soluble cancer therapeutics that are not capable of being administered in typical aqueous excipients.^[63–66] Furthermore, due to their relatively small size, micellar formulations are substantially extravasated from blood vessels to the deep tumor tissues, enabling their uniform distribution over the entire tumor.^[67,68]

Since many magnetic or optical nanocrystals are synthesized in organic phases, [6,69-73] methods had to be developed to enhance water solubility to improve compatibility in biological media. The first demonstrations of *in vitro* imaging with

semiconductor quantum dots occurred in 1998,[74,75] and in 2002 quantum dots coated with a micellar overlayer were shown to be soluble and stable enough for both in vitro and in vivo imaging.^[76] With the more recent development of micellar coatings consisting of block-copolymers, numerous hydrophobic nanocrystals have been successfully modified and solubilized for biological applications.[77-86] Some of these have demonstrated dual imaging modes (fluorescence imaging and MRI) by incorporating a fluorescent or paramagnetic molecular species into the lipid that covers either a magnetic or luminescent nanocrystal, respectively. Alternatively, both types of nanocrystals have been incorporated into a more conventional micelle.[77,85-88]

Micellar hybrid nanosystems have also been used to co-incorporate functional nanocrystals (for imaging) and therapeutic agents (Table 4). Hydrophobic nanocrystals can be incorporated in the central region of a micellar nanodevice, [89,90] while hydrophilic nanocrystals can be conjugated to the surface of a micellar nanodevice. [91] Jain et al. developed a novel micellar hybrid nanosystem where poorly soluble therapeutic molecules partitioned into the hydrophobic shell surrounding the magnetic nanocrystals on the interior of the micelle. The drugs were secured at the interface with a polyethylene oxide amphiphile (Pluronic, polyoxyethylene-polyoxypropylene triblock copolymer), which conferred aqueous solubility to the hybrid. [92,93] The researchers demonstrated sustained release of the incorporated chemotherapeutics *in vitro* for 2 weeks. Additionally, the micellar magnetic nanoparticles exhibited a significant MR signal in the carotid arteries of mice after intravenous injection. Prasad and co-workers designed a similar multifunctional polymeric micelle-based nanocarrier system that consists of polymeric micelles of diacylphospholipid-poly(ethylene

glycol) (PE-PEG) co-incorporated with the hydrophobic photosensitizer drug 2-[1-hexyloxyethyl]-2-devinl pyropheophorbide-a (HPPH) and magnetic nanocrystals. [94] Hydrophobic interactions between the hydrocarbon chains of PE-PEG and the hydrocarbon coating on the magnetic nanocrystals stabilized the micellar nanocarriers and enhanced the loading of the hydrophobic drug. It was observed that the efficacy of photosensitization is not altered in the micellar assemblies. The hybrid nanocarriers could magnetically deliver photosenitizer agents into tumor cells *in vitro*, resulting in enhanced internalization and phototoxicity. The pH-sensitive micellar hybrid nanoparticles have been also utilized to effectively release an encapsulated therapeutic payload in acidic lysosomes of the cell while simultaneously monitoring their intracellular distribution. [95,96]



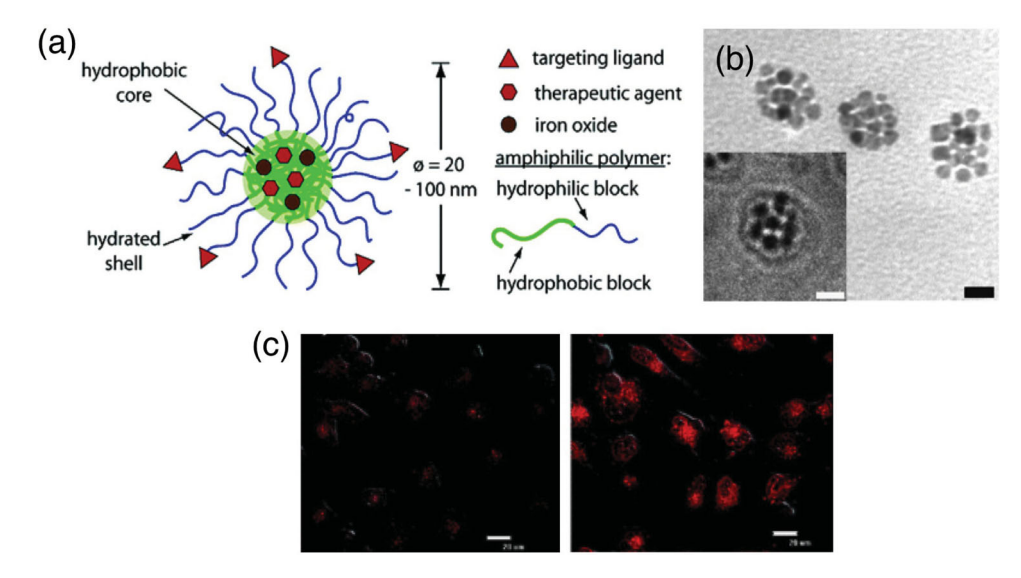


Figure 3. a) Schematic design of polymeric micellar hybrid nanoparticles, where the micellar membrane is composed of amphiphilic block copolymers. The targeting ligand is cyclic RGD and the therapeutic agent is doxorubicin (DOX). The hydrophobic core also contains superparamagnetic iron oxide (Fe₃O₄) nanoparticles to enable magnetic resonance imaging. b) Transmission electron microscope (TEM) image of the polymeric micellar assembly. The inset is a cryo-TEM image of the same micelle formulation. Scale bars are 20 nm. c) Confocal laser scanning microscope image of human Kaposi's sarcoma SLK cells treated with polymeric micelles either with (right panel) or without (left panel) a cRGD targeting peptide. The intrinsic fluorescence of the DOX drug appears as red in the images. Scale bars are 20 μm. Reproduced with permission from ref. [97] Copyright © 2008 American Chemical Society.

Gao and co-workers reported substantial cancer-targeting capability of multifunctional polymeric micelles that contain molecular drugs and MRI contrast agents (Figure 3).[97,98] The hydrophobic core region of a single micelle was co-loaded with a cluster of magnetic nanocrystals and the anti-cancer drug doxorubicin. Interestingly, a micellar nanostructure composed of amphiphilic block copolymers of poly-(ethylene glycol)block-poly(D,L-lactide) (PEG-PLGA) copolymer was observed to release the incorporated drug to cells more rapidly relative to micelles that used poly(ε -caprolactone) (PCL) as the hydrophobic core constituent.^[64] Furthermore, hybrid micelles with attached cRGD targeting ligands delivered the incorporated therapeutics more efficiently to integrin $\alpha_{\nu}\beta_{3}$ -expressing tumor cells. Recently, Namiki and co-workers demonstrated that lipid-coated magnetic nanocrystals (LipoMag) exhibited more efficient gene silencing and better anti-tumor effects after magnetically guided targeting than commercially available polymer-coated nanocrystals (PolyMag).[99] This micellar coating that led to solubilization of individual hydrophobic magnetic nanocrystals enabled LipoMag to prolong their circulation in the blood and efficiently deliver the incorporated siRNA to the tumor site compared with a larger PolyMag formulation composed of irregularly shaped magnetic clusters. In addition, a pH-sensitive micellar layer encapsulating magnetic nanocrystals and a therapeutic cargo allowed the MRI-detectable nanostructure to release its payload selectively in an acidic environment of the tumor.[100,101] These works demonstrate the potential of micellar hybrids as theranostic agents—for targeted systemic administration of therapeutic molecules while simultaneously allowing MR imaging.

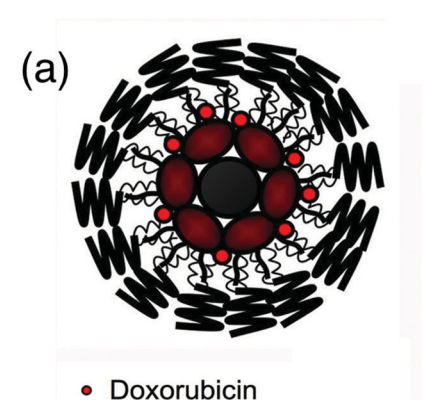
The above examples illustrate the power of the micellar encapsulation approach: it allows one to incorporate multiple,

distinctively different payloads within a single nanostructure.[102] It also allows the administration of theranostic combinations that can provide complementary or confirmatory information, for example in MRI and fluorescence imaging. We and others have synthesized hybrid nanoparticles that contain magnetic nanocrystals, quantum dots and a molecular anti-cancer agent within a single poly(ethylene glycol)-phospholipid micelle (Figure 4).[19] The two different types of hydrophobic nanocrystals were incorporated with doxorubicin during synthesis, and their targeted delivery to tumor cells was demonstrated using a pendant targeting peptide. The dual-mode imaging (by MRI and fluorescence) of a xenografted tumor in a mouse was demonstrated. The work illustrated the ability to combine optical with magnetic resonance imaging, to obtain microscopic resolution at the tumor site by fluorescence, and full anatomical distribution by MRI.

Micellar coatings have also been employed to separately control release of two different drugs co-encapsulated into a hybrid nanoparticle. Sasisekharan and co-workers fabricated a novel micellar nanosystem, which they named a "nanocell" that comprises a poly-(lactic-co-glycolic) acid (PLGA) polymeric nanoparticle core within a PEGylated-lipid shell. [103] Once the nanocells accumulate in a tumor after systemic administration (mouse model), the outer shell first releases an anti-angiogenic agent, causing vascular shutdown, and then the polymeric core, which is presumably trapped in the tumor upon vascular shutdown, releases its chemotherapeutic agent. The "one-two punch" very elegantly illustrated by this work demonstrates a key advantage of nanotechnology—it provides an ability to incorporate hierarchical, synchronized functions into an injectable formulation.



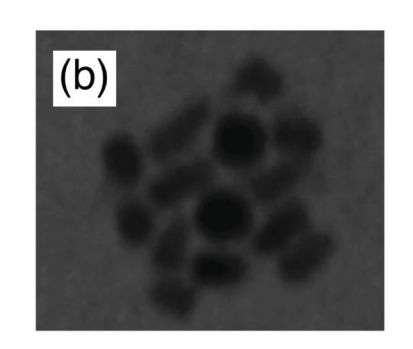
www.advmat.de

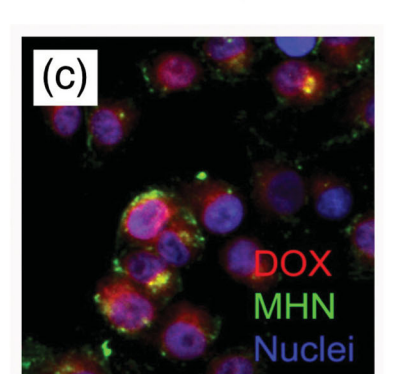


Quantum dot

PEG-phospholipid

Magnetic nanoparticles





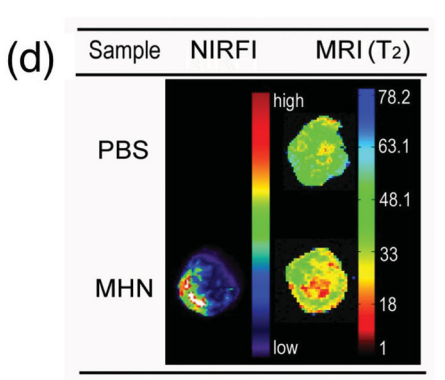


Figure 4. a) Schematic representation of micellar hybrid nanoparticles containing two different types of nanoparticles and a molecular drug. b) Transmission electron microscope (TEM) image of a micelle containing a mass ratio of 1 magnetic nanoparticle for every 3 quantum dots. The scale bar is 100 nm. In these formulations the quantum dots are elongated and the magnetic nanoparticles are spherical. c) Fluorescence microscope image showing targeted delivery of doxorubicin (DOX)-incorporated micelles to MDA-MB-435 human carcinoma cells. The micelles have peptide targeting groups attached to their surface. d) MRI and NIR fluorescence images of tumors harvested from mice 20 h after injection with the micellar nanostructures ("MHN"). Control is injection with phosphate buffered saline ("PBS"). Reproduced with permission from ref. [19] Copyright 2008 Wiley VCH.

2.3. Porous Silica-Based Hybrid Nanoparticles

Mesoporous silica nanoparticles are another class of "hollow" nanoparticles that have attracted great attention as potential drug carriers due to their large surface area, tunable size and porosity, chemical stability and biocompatibility. [12,104] The synthesis of mesoporous silica is based on the formation of liquid-crystalline mesophases of amphiphilic molecules (surfactants) that serve as templates for the *in situ* condensation of orthosilicic acid. [13] Mesoporous silica nanospheres have been shown to be readily taken up by eukaryotic cells without any significant cytotoxicity, and their internalization can be manipulated by surface functionalization of the nanoparticles. [12,105–107] Additionally, magnetic or fluorescent imaging molecules can be easily incorporated using well-developed silane and silanol chemistries. [108–114] These formulations are also capable of hosting a wide variety of therapeutic molecules. [108,109,115–117]

The molecules can be coupled to the inner surface of mesoporous silica nanoparticles via pH-sensitive linkers for controlled release in lysosomes.[118] For example, Lin and coworkers trapped genes along with their chemical inducers inside silica mesopores using gold nanoparticle caps.[115] These therapeutic systems were able to release their payload and trigger gene expression in a plant model (tobacco mesophyll protoplast). The same group described other types of hybrid mesoporous silica nanosystems that achieve tunable release of therapeutics using nanoparticle-based capping reactions.[105,109] If the capping nanoparticle is a magnetic nanocrystal, it can be used to manipulate the hybrid delivery nanosystem and release the encapsulated molecules under magnetic actuation in addition to serving a blocking function.[109,119]

Another approach is to encapsulate other types of nanoparticles within a shell of mesoporous silica where therapeutic molecules can be incorporated (Table 5). The therapeutic molecule incorporated in the mesoporous silica layer is protected from degradation in the physiological environment. Several groups have reported that magnetic nanocrystals or quantum dots can be coated with a layer of porous silica. [20,120–129] These magnetic or optical drug carriers with a porous shell have been mainly used to demonstrate magnetic separation, MR/optical imaging and drug delivery both in vitro and in vivo. Shi and co-workers fabricated uniform magnetic nanospheres composed of an Fe₃O₄ iron oxide core and a mesoporous silica shell.[121] The mesoporous silica shell was formed on a single magnetic nanocrystal by simultaneous sol-gel polymerization of tetraethoxysilane (TEOS) and n-octadecyltrimethoxysilane (C18TMS) followed by removal of the

organic groups. Hyeon and co-workers enabled precise control of particle size and silica shell thickness in core-shell magnetic mesoporous silica nanoparticles by varying the concentration of the cetyltrimethylammonium bromide (CTAB)-coated core magnetic nanocrystals during the silica condensation reaction (Figure 5).[20] The nanoparticles were made fluorescent by attachment of fluorescein or rhodamine dyes via a 3-aminopropyltriethoxysilane (APTES) linker. In vitro drug delivery and multimodal imaging were first successfully demonstrated using these uniform multimodal nanocarriers. Furthermore, significant passive tumor accumulation of the nanocarriers was observed after intravenous injection, demonstrating their excellent in vivo stability. Mesoporous silica coatings can also be applied to CTAB-coated gold nanorods using similar procedures.[130-132] Zhang and co-workers have developed a therapeutic nanodevice where NaYF4 up-converting nanocrystals were encapsulated with a uniform layer of mesoporous silica

-11

www.MaterialsViews.com

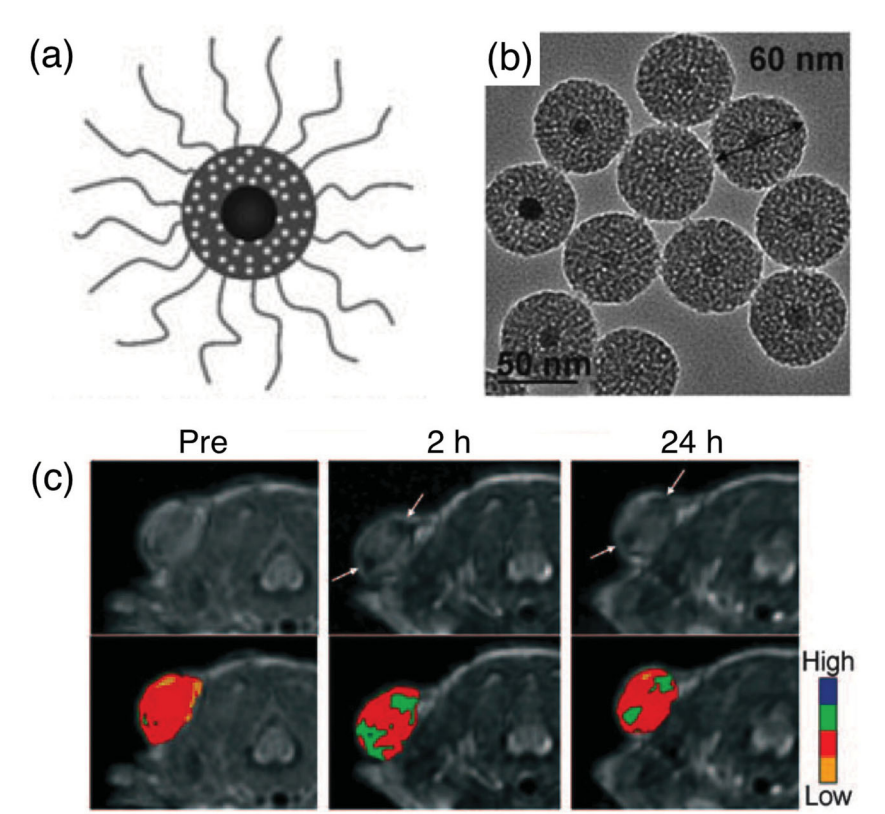


Figure 5. a) Schematic depiction of porous silica-coated magnetic hybrid nanoparticles containing a poly(ethylene glycol) (PEG) overcoating. b) Transmission electron microscope (TEM) image of the nanostructures, showing monodispersed magnetic nanocrystals coated with a uniform mesoporous silica shell. c) *In vivo* T₂-weighted MR images (upper row) and color maps (lower row) of an MCF-7 tumor implanted on a nude mouse before and after intravenous injection of the nanoparticles (5 mgFe/kg). The arrows indicate regions of enhanced MR contrast resulting from accumulation of nanoparticles in the tumor (by the EPR effect). Reproduced with permission from ref. [20] Copyright 2008, Wiley VCH.

that contained a zinc phthalocyanine photosensitizer.^[133] The nanocrystals activated the incorporated photosensitizer upon excitation with a NIR laser in order to release reactive singlet oxygen as a cancer chemotherapeutic.

To achieve more efficient loading of therapeutic molecules into the pores, functional nanocrystals have been attached to the surface of mesoporous silica nanoparticles (Table 5). Hyeon and co-workers reported porous silica-based multifunctional nanoparticles that incorporated drugs into their porous interior and magnetic nanocrystals on their surface. [134] *In vivo* passive accumulation of the hybrid nanoparticles in the tumor region was imaged with the MRI-active nanocomponents. Furthermore, the anti-cancer drug doxorubicin incorporated into the pores of the hybrid nanoparticle was also efficiently localized in the tumor region. Immobilization of therapeutic molecules on their inner wall via pH-responsive hydrazone bonds enabled more effective release of the incorporated molecules to the cytoplasm from the nanoparticle. [135]

Mesoporous silica nanoparticles have been used to encapsulate both functional (magnetic or optical) nanocrystals and drugs in their porous nanostructure (Table 4). Brinker and co-workers have developed a hybrid nanostructure composed of a mesoporous silica nanoparticle core with a lipid bilayer shell.^[136] The

hybrid is prepared by fusion of a positively charged liposome on a negatively charged mesoporous silica nanoparticle. Interestingly, this electrostatic arrangement allows the loading of a negatively charged drug into the nanohybrid. Furthermore, they demonstrated that calcein, which is membrane impermeable and fluorescent, is incorporated into the liposomal porous nanoparticles and then released in the endosomal compartments of cells, where the localized pH is significantly lower (~5) than in the extracellular media (~7). Compared with conventional liposomes, the stability of the lipid coating on the rigid silica scaffold allows more effective loading and sustained release of a drug. Recently, the liposome-coated nanoporous particles with enormous loading capacity were further decorated with a targeting peptide that binds to human hepatocellular carcinoma and incorporated with multicomponent cargos (both therapeutic molecules and quantum dots).^[137] The targeted delivery of a drug cocktail with the lipid-coated porous nanoparticles enabled effective destruction of drug-resistant human hepatocellular carcinoma cells.

Recently, several research groups have developed porous silica "nanorattles" consisting of a hollow nanoparticulate shell containing various materials in the interior. These structures can effectively incorporate a large amount of therapeutic payload into the empty inner space. [138–140] Tang and coworkers have fabricated multifunctional silica nanorattles coated with a gold nanoshell for the combination of photothermal therapy and

chemotherapy.^[141] This dual cancer treatment with gold-coated silica nanorattles showed enhanced overall therapeutic efficacy and reduced systemic toxicity. Stucky and co-workers have developed mesoporous multifunctional upconverting luminescent and magnetic nanorattles for targeted optical imaging and chemotherapy.^[142] The magnetic nanocrystals and therapeutic molecules were both incorporated into the hollow interior of the upconverting luminescent rare-earth-doped NaYF₄ nanorattle shell. These multifunctional nanorattles were guided through the influence of an external magnetic field to the tumor region, providing an improved anti-cancer outcome. Their localization in the tumor was monitored with the visible luminescence from the nanorattle, induced by 2-photon NIR excitation.

2.4. Polymeric Hybrid Nanoparticles

Biodegradable polymeric nanoparticles derived from poly(D,L-lactic-co-glycolic acid) (PLGA) have been widely used for a variety of biological applications due to their biocompatibility (FDA-approved components) and their ability to encapsulate and provide controlled release of drugs.^[103,143–151] PLGA nanoparticles containing relatively high loadings of a molecular

www.advmat.de

cargo can be prepared by arrested precipitation and water-in-oilin-oil (W/O/O) double emulsion techniques.[152,153] In addition to drugs, the use of imaging contrast agents as a cargo has been of interest. Brannon-Peppas and co-workers developed Gdloaded polymeric nanoparticles for T₁-weighted MR imaging, in this case focused on atherosclerosis detection. [154] The waterin-oil-in-oil double emulsion solvent evaporation method allows high loading of diethylenetriaminepentaacetic acid gadolinium (III) (Gd-DTPA), an FDA-approved positive MR contrast agent, in PLGA nanoparticles. The longitudinal relaxivity (r_1) of the particle formulation was shown to be similar to that of unencapsulated Gd-DTPA. Feng and co-workers developed a PLGA nanoparticle system containing magnetic nanocrystals for MR imaging.[155] Similar to the micellar systems, the superparamagnetic properties of the hybrids are significantly enhanced relative to individual magnetic nanocrystals due to the close proximity of the magnetic nanoparticles, improving the MR contrast effects. Ex vivo MR images of livers from mice injected with the hybrids or with singular magnetic nanocrystals were compared to confirm the MR contrast enhancement achieved by placing multiple magnetic nanocrystals in close proximity. Magnetically-guided drug delivery and other biomagnetic applications were also demonstrated with these systems. [156]

Combinations of functional nanocrystals (fluorescent quantum dots or MRI-visible magnetic nanoparticles) and therapeutic agents have been found to be compatible with polymeric nanoparticles (Table 6).^[157–160] Desai and co-workers synthesized biodegradable and surfactant-free nanoparticles co-incorporated with hydrophobic drug, Coenzyme Q10, and quantum dots using an arrested precipitation method.[161] Hyeon and coworkers synthesized a similar multifunctional polymer system co-encapsulated with a hydrophobic therapeutic agent (doxorubicin) and either hydrophobic superparamagnetic nanocrystals or hydrophobic quantum dots, using an oil-in-water emulsion and a subsequent solvent evaporation technique. [162] The preparation provides polymeric hybrid nanoparticles with uniform shapes in the size range of 100-200 nm. For targeted imaging and therapy, a folate group was coupled onto the surface of the polymeric hybrid nanoparticles. The folate-conjugated polymeric hybrid nanoparticles enabled effective targeted delivery of therapeutic agents to the folate receptor-positive KB cancer cells, which could be detected by optical (quantum dots) and MR (magnetic nanocrystals) imaging techniques. Recently, coincorporation of magnetic nanocrystals and the anti-cancer drug doxorubicin into a single thermosensitive polymeric nanodevice was demonstrated for theranostic applications.^[163] The encapsulated drug was released selectively in response to the physiological temperature by de-swelling of the polymeric nanodevice.

Plasmon-induced photothermal activation of a gold nanostructure is often used to induce payload release from a polymeric nanodevice (Table 6). Yoo and co-workers introduced multifunctional hybrid nanoparticles combining photothermally controlled drug delivery with MR imaging in a polymeric host. ^[164] The polymeric nanoparticles were composed of PLGA, prepared with half-shells of metal multilayers (Mn and Au) that were resonant in the NIR region of the spectrum. The authors harnessed the known ability of PLGA to release loaded drugs more rapidly with increasing temperature. ^[165] NIR light absorbed in the metallic layers was converted to thermal energy,

which then induced degradation of the polymeric core and released the incorporated drugs. The nano-assemblies also displayed enhanced MRI contrast. Drug delivery from such gold-based hybrid nanoparticles can be synergistically combined with hyperthermia and molecular imaging, thus enhancing the efficacy of cancer therapy. For example, the same group recently demonstrated complete destruction of tumors in a mouse model using metal multilayer/PLGA nanoparticle constructs. [166,167] Tumor destruction derived from a combination of hyperthermia and targeted drug delivery.

There are several examples of polymeric hybrid nanoparticle systems aimed at in vivo simultaneous drug delivery and imaging (Table 6).[168-170] Shi and co-workers developed a multifunctional nanocarrier system where superparamagnetic Fe₃O₄ nanocrystals and chemotherapeutic agent paclitaxel were co-loaded into the biodegradable polymeric nanomatrix and quantum dots and targeting antibodies were attached to its surface.[171] Significant targeting of these multifunctional nanocarriers to xenografted prostate tumors in a mouse was observed with multiple imaging modalities. Haam and co-workers developed polymeric nanohybrids consisting of magnetic nanocrystals and anticancer drugs encapsulated in an amphiphillic block copolymer (PEG-PLGA) using a nanoemulsion method (Figure 6).[172] Incorporation of a large amount of magnetic nanocrystals (~ 40 wt%) into the polymeric hybrid nanoparticles enabled ultrasensitive T2-weighted MR imaging. The encapsulated drug doxorubicin was slowly released over 2 weeks from the hybrid nanoparticles, presumably owing to polymer degradation and dissolution. A targeting group was attached to the surface of these hybrid nanoparticles in the form of an antibody against human epidermal growth factor receptor 2, which is a targeting marker for the treatment of patients with metastatic breast cancer. The antibody-conjugated polymeric hybrid nanoparticles allowed for targeted detection of cancer both in vitro and in vivo (by MR imaging), and the drug-loaded targeted nanocarriers demonstrated significant therapeutic efficacy against both cancer cells in vitro and xenografted tumors in vivo (mouse model).

2.5. Viral Hybrid Nanoparticles

A variety of viruses have been successfully re-engineered to act as synthetic nanoparticles for biological applications. Compared with most other synthetic nanoparticles, viral nanoparticles are more uniform in size and shape, they can better protect therapeutic nucleic acid payloads, and they can deliver these payloads into cells and tissues with greater selectivity. Their biological selectivity is easily optimized; manipulation of their genome can be used to modify the functional moieties displayed on the viral nanoparticle surface. These species may have their own specific targeting capabilities, or they may serve as sites for attachment of additional targeting ligands. The protein coating (capsid) of viral nanoparticles also allows for encapsulation or conjugation of non-nucleic acid therapeutic payloads—small molecules or proteins—for targeted delivery. The protein coating delivery.

In the past few years, several examples of hybrid viral nanoparticles have been developed to monitor biological functions either *in vitro* or *in vivo* (Table 7). Magnetic nanocrystals have

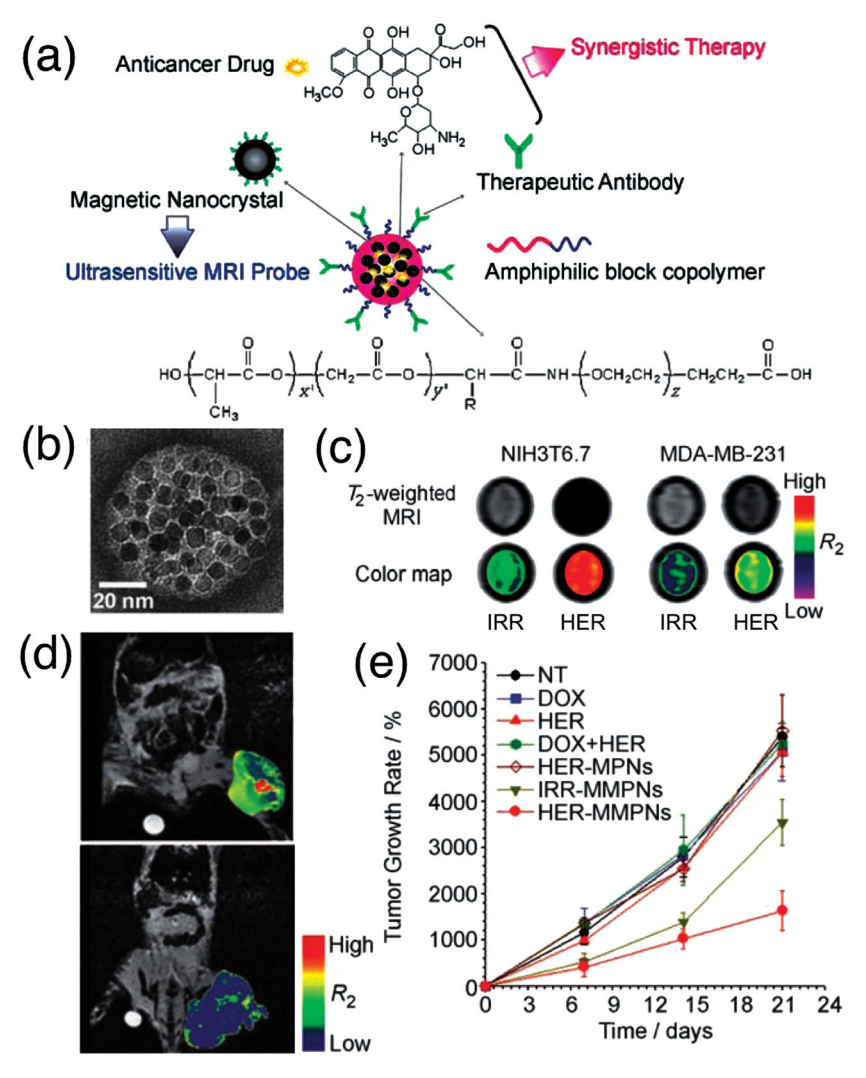


Figure 6. a) Schematic depicting the fabrication of multifunctional magneto-polymeric nanohybrids (MMPNs), a hybrid nanoparticle in which the main structure comprises a polymer, into which are embedded magnetic MnFe₂O₄ nanocrystals. b) Transmission electron microscope (TEM) image reveals a high loading of MnFe₂O₄ nanocrystals. c) T₂-weighted MR images (upper row) and intensity color maps (lower row) of NIH3T6.7 and MDA-MB-231 cells treated with nanoparticles containing an irrelevant antibody (IRR) or an antibody specific to human epidermal growth factor receptors (HER). d) *In vivo* MR images and corresponding intensity color map of mice bearing NIH3T6.7 tumors 1 h after intravenous injection of HER-labeled (upper panel) and IRR-labeled (lower panel) nanoparticles. e) Comparative therapeutic efficacy study in mice shows a significant reduction in the rate of growth of NIH3T6.7 tumors treated with the HER-labeled nanoparticles containing the anti-cancer drug doxorubicin, compared with free doxorubicin or other controls. Reproduced with permission from ref. [172] Copyright © 2008 Wiley VCH.

been coupled to the exterior of the capsid of viral nanoparticles for MRI visualization.^[183–185] Magnetically-guided gene delivery has been accomplished with viral nanoparticles containing superparamagnetic iron oxide nanoparticles.^[186–188] To image viral nanoparticles at a higher resolution, quantum dots have been placed either on the surface of or inside viral nanomaterials.^[189–193] Additionally, the protein constituents of viral nanoparticles have been self-organized onto the surface of an inorganic spherical nanoparticle (magnetic or gold nanocrystal).^[194–197]

The extensive and selective transfection of cells that can be accomplished with viral nanoparticles provides the potential for effective gene therapy against genetic diseases and cancer.[198] Recently, there have been intensive efforts to integrate both diagnostic and therapeutic functions into a single viral hybrid nanosystem. Cheon and co-workers hybridized a viral nanoparticle with magnetic nanocrystals for simultaneous targeted gene delivery and MR imaging (Figure 7).[199] In that work, magnetic nanocrystals with a monodisperse size of 12 nm were conjugated to an adenovirus that displayed selectivity to cells that over-express Coxsackievirus B adenovirus receptor (CAR). The magnetic viral nanoparticles readily internalized into the CAR-positive cells, and these cells were then selectively detected by MR imaging. The CAR-mediated infection by the hybrid nanoparticles also allowed efficient and selective gene delivery. This was demonstrated using genes that code for eGFP (enhanced green fluorescent protein); the targeted cells expressed this readily detected fluorophore.

Curiel and co-workers incorporated a second function to a gene-delivering nanoparticle by modifying adenoviral vectors with excitable gold nanoparticles—thus allowing both targeted gene therapy and hyperthermia with the same targeted nanoparticle. [200] Gold nanoparticles were covalently conjugated to lysine residues on an adenovirus capsid encoding a luciferase reporter gene. Goldlabeled adenoviral vectors with a gold:virus ratio of 100:1 retained their ability to infect HeLa cells, although higher conjugation ratios significantly reduced infectivity. Since the primary receptor of adenoviral vectors, the Coxsackie adenovirus receptor (CAR) is not a highly effective target for most human tumors, gold-labeled adenoviral vectors were re-engineered to target human cancer cells by reacting them with a fusion protein. These gold-labeled adenoviral vectors displayed similar luciferase expression to unmodified adenoviral vectors in MC38-CEA-2 cancer cells. Recently, additional examples of photo-activatable viral nanoparticles have been devel-

oped for targeted photothermal heating/imaging by decorating a virus capsid with C_{60} ("buckyballs")^[201] or by encapsulating a gold nanoparticle with viral proteins.^[202]

Belcher and co-workers have developed genetically engineered multifunctional M13 bacteriophages assembled with fluorescent carbon nantubes.^[203] The filamentous M13 bacteriophages can display material-specific peptides and/or targeting motifs on their capsid using genetic engineering. The single-walled carbon nanotubes were selectively coupled to the genetically engineered bacteriophages for NIR fluorescence imaging





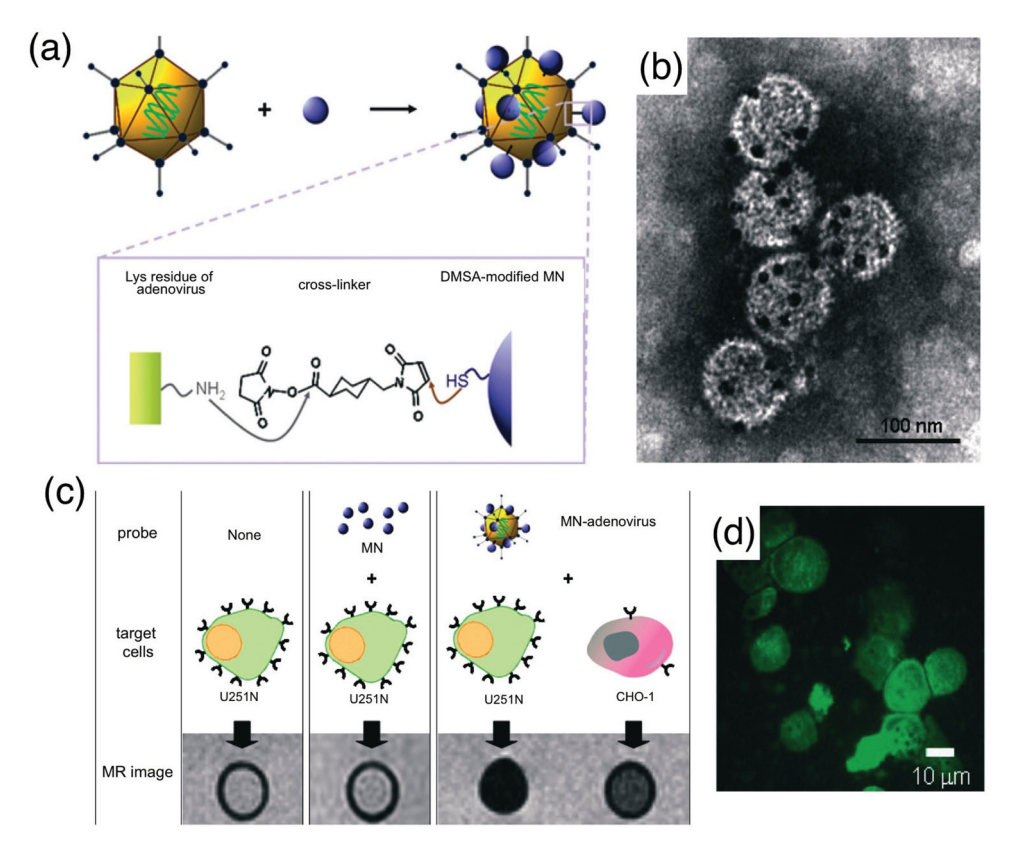


Figure 7. a) Schematic of viral nanoparticle hybrids consisting of magnetic nanocrystals (MN) attached to an adenovirus nanoparticle. b) Transmission electron microscope (TEM) image of the construct. Scale bar is 100 nm. c) T₂-weighted MR images of untreated U251N cells, MN-treated U251N cells, MN-adenovirus treated U251N cells, and MN-adenovirus treated CHO-1 cells. d) Fluorescence microscope image of U251N cells treated with MN-adenovirus containing a gene that codes for eGFP (enhanced green fluorescent protein). Expression of the delivered gene causes the cells to emit the fluorescence characteristic of eGFP. Reproduced with permission from ref. [199] Copyright © 2007 Wiley VCH.

of tumors. These multifunctional bacteriophages were effectively accumulated in the tumor and their targeting was clearly imaged by NIR fluorescence from the carbon nanotube in a separate spectral window. These bacteriophage vectors can be further genetically modified to treat cancer using targeted gene therapy by inserting therapeutic genes into the vector backbone and displaying targeting ligands on the vector surface.

2.6. Gold-Based Hybrid Nanoparticles

Gold nanoparticles display very unique optical properties originating from plasmons—collective oscillations of highly mobile electrons resident in the metal at optical frequencies. One of the most important properties of plasmonic systems is their very large absorption cross-section relative to molecule or semiconductor-based absorbers. This allows the efficient coupling of external optical fields into photoemissive, thermal, or chemical effects. Gold-based plasmonic nanostructures have been widely utilized for cancer diagnostics and therapy.^[204] They have become promising contrast agents for biological imaging such as computed tomography (CT),^[205–208] optical coherence tomography (OCT),^[209–212] two-photon-induced photoluminescence (TPIP),^[213,214] photoacoustic imaging,^[215,216] silver-enhanced

staining^[217,218]), and surface enhanced Raman spectroscopy (SERS).^[219–223] In addition, gold-based nanoparticles such as nanorods, nanocages and nanoshells have been of great interest for photothermal therapy due to their strong and tunable linear absorption in the near-infrared (NIR) region where tissue penetration can be maximized.^[14,15,209,224–229] Lastly, since colloidal gold has been long used to treat rheumatoid arthritis in humans,^[230] the biosafety of gold-based nanoparticles is currently well accepted, even though the material may not degrade completely *in vivo*.^[231,232]

Simultaneous biological imaging and photothermal therapy could be achieved using gold-based hybrid nanoparticles (Table 8). [18,233–240] Hyeon and co-workers designed multifunctional magnetic gold hybrid nanoparticles consisting of a silica nanosphere core surrounded by a gold nanoshell for photothermal therapy, with embedded magnetite nanoparticles for T_2 MRI contrast enhancement (**Figure 8**). [18] Both magnetic nanocrystals of 7 nm and gold seed nanoparticles of 1–3 nm were first attached to aminated silica nanospheres. A gold nanoshell was then uniformly grown around the silica nanosphere. Absorbance spectra ranged from 700 nm to the NIR, a suitable spectral region for photothermal therapy due to the relatively deep penetration of NIR radiation in biological tissues. After linking to anti-HER2/neu targeting moieties, the

Makrials Views

www.MaterialsViews.com

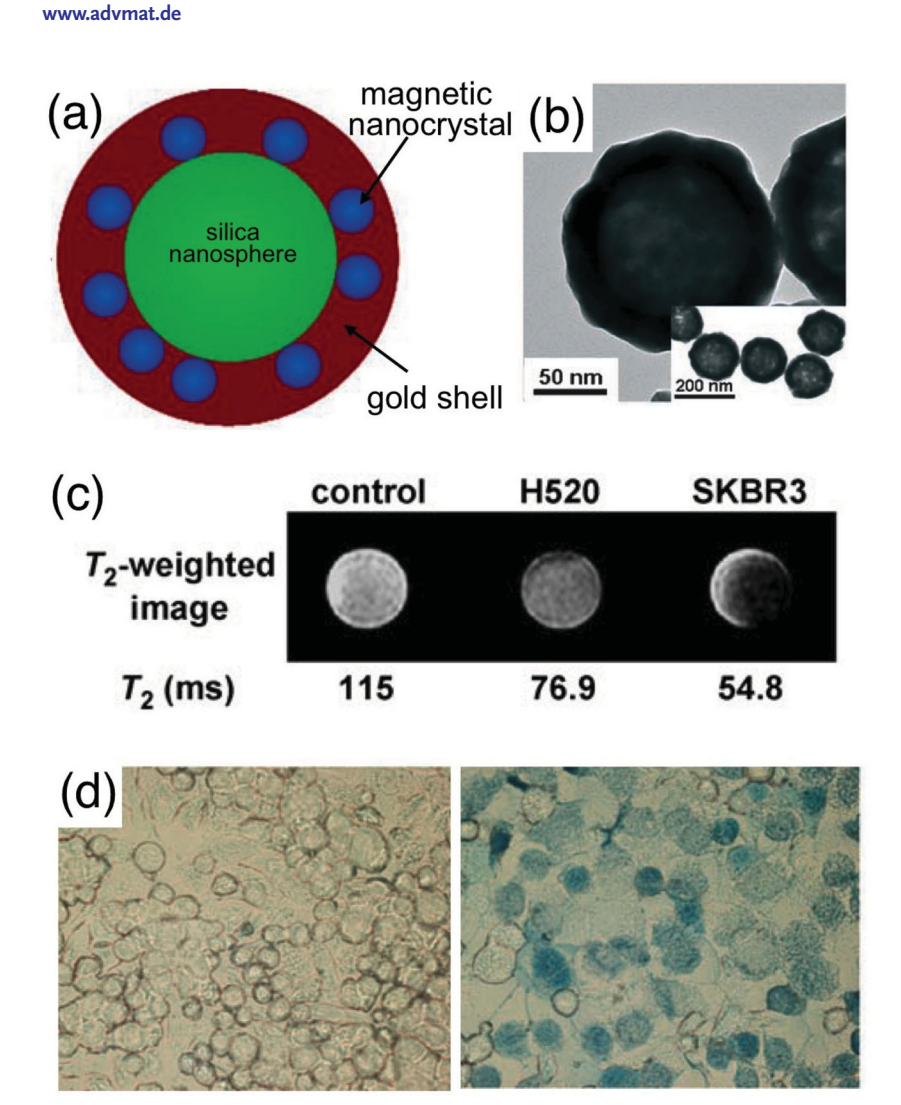


Figure 8. The "core-shell" motif is common in hybrid nanoparticle design. a) In this example, the shell consists of a gold layer that also contains magnetic nanoparticles. This two-component shell encapsulates a silica core (Mag-GNS). The presence of both the magnetic component (iron oxide) and the plasmonic component (gold) allows imaging (by MRI) and hyperthermia (by laser heating), respectively. b) Transmission electron microscope (TEM) image of Mag-GNS. c) *In vitro* T₂-weighted MR images of control SKBR3 cells, HER2/*neu*-negative H520 cells treated with AbHER2/*neu*-coupled Mag-GNS, and HER2/*neu*-positive SKBR3 cells treated with AbHER2/*neu*-coupled Mag-GNS. The corresponding T₂ relaxation times are indicated below the MR images. d) Optical microscope images of control SKBR3 cells (left panel) and SKBR3 cells treated with AbHER2/*neu*-coupled Mag-GNS (right panel) after irradiation for 10 s with a femtosecond-pulsed laser (operating at a wavelength of 800 nm). A trypan blue stain reveals the large quantity of dead cells resulting from the treatment. Reproduced with permission from ref. [18] Copyright © 2006 Wiley VCH.

hybrid nanoparticles selectively interacted with cancer cells and the targeted cells were detected by T₂-weighted MR imaging. Furthermore, the cancer cells targeted with the hybrid nanoparticles could be thermally ablated upon short exposure to NIR radiation. Li and co-workers synthesized bifunctional gold nanoshells with a superparamagnetic iron oxide-silica core for both MR imaging and photothemal therapy.^[235] The iron oxide nanocrystal was first coated with an amorphous silica layer via the sol-gel process and the surface of the silica layer was further functionalized with amine groups. As mentioned earlier, gold nanocrystal seeds (2–3 nm) could then be attached to the silica

surface and used to nucleate the growth of a gold shell on the silica surface. The middle layer of silica containing hybrid nanoparticles provided a dielectric interface for shifting the plasmonic resonance to the NIR region, as has been done with the more conventional gold nanoshell constructs.[225] Irudayaraj and co-workers have fabricated multifunctional nano-pearl-necklaces where multiple iron oxide nanocrystals were linked on the surface of a single gold nanorod.[236] This multifunctional nanocomplex, conjugated to Herceptins, allowed for targeted dual-mode imaging (MRI with magnetic nanocrystal and two-photon luminescence with gold nanorod) and therapy (photothermal heating with gold nanorod) of cancer cells. Recently, Liu and co-workers developed multifunctional upconversion nanoprobes for multimodal imaging and dual-targeted photothermal therapy.^[241] The luminescent upconverting nanocrystals used as a core material of the hybrid nanoparticle system offered effective optical imaging with NIR light excitation while magnetic nanocrystals and gold nanoshells placed on the surface of the hybrid nanoparticle enabled MR imaging, magnetic targeting, and photothermal therapy. These multifunctional nanoprobes homed to tumors with dual (magnetic and ligand) targeting strategies, and they allowed multimodal imaging of the tumor targeting process (with upconversion luminescence and MRI), as well as the selective photothermal treatment of tumors. These hybrid nanoparticles possessed superparamangetic characteristics for MR imaging and magnetic actuation and strong absorbance in the NIR region of the electromagnetic spectrum for photothermal therapy.

2.7. Nanotube-Based Hybrid Nanoparticles

Carbon nanotubes are hydrophobic, tubular nanostructures with diameters on the order of a few nanometers that display remarkable mechanical and optical properties. [242,243] These characteristics have been harnessed in

biomedical applications such as diagnostic imaging (fluorescence, Raman and photoacoustic), [244-253] drug delivery, [248,254-260] and photoablative therapy. [244,261-264] Carbon nanotubes administrated systemically into mice have been reported to be nontoxic and excretable via either renal or biliary pathways depending their surface chemistries, although excretion requires a long time relative to many other nanoparticles. [265-267]

Several types of magnetic hybrid carbon nanotubes have been developed for magnetic actuation and MR imaging in recent years (Table 8).^[268–273] Iijima and co-workers demonstrated *in vivo* MR imaging using single-walled carbon "nanohorns" (one

ADVANCED MATERIALS

www.advmat.de

www.MaterialsViews.com

type of carbon nanotube with 40 nm long, 2-5 nm in diameter, and at least one end closed by a conical cap) labeled with magnetite nanocrystals.^[274] The hybrid nanohorns were prepared by deposition of Fe(OAc)2 on oxidized carbon material and subsequent heating to 400 °C. The process results in strong attachment of the superparamagnetic magnetite nanocrystals to the carbon nanohorns, which enabled T2-weighted MR imaging of the hybrids in the spleen and kidneys of living mice. Preliminary in vivo toxicity tests indicated that the hybrid nanohorns were biocompatible at doses up to 8 mg/kg body weight. Strano and co-workers introduced asymmetric single-walled carbon nanotube/iron oxide nanoparticle complexes as multimodal biomedical imaging agents.^[275] Their synthesis places ~3nmdiameter magnetic nanocrystals at only one end of the nanotube and the surface of the assembly is stabilized with oligonucleotides. This nanocomplex displayed distinctive NIR luminescence signatures from the single-walled carbon nanotubes. The hybrids were shown to internalize into macrophage cells. and both MR and NIR fluorescence modalities could be used to image them. The intrinsic photothermal properties of the nanotubes allowed MR-guided photothermal treatment of tumors in a mouse xenograft model. [276]

Although carbon nanotubes can display intrinsic NIR luminescence, [250,252] the natural intensity of this process is generally too weak to achieve whole-body imaging *in vivo*. Shi and co-workers developed luminescent multi-walled carbon nanotubes labeled with quantum dots in an effort to overcome

this limitation.^[277] Multi-walled carbon nanotubes possessing a larger inner volume relative to single-walled carbon nanotubes were chosen for this study, to allow incorporation of anti-cancer drugs. A plasma polymerization technique was employed to place thin films of functional groups on the nanotube surface to provide a means to attach quantum dots. The resulting nanotubes displayed strong emission in the visible spectrum, which was harnessed to report their anatomical location in a mouse. Rusling and co-workers added cisplatin to the quantum dot-carbon nanotube assemblies, and demonstrated a positive therapeutic effect in a mouse xenograft tumor model (Figure 9).[278] When decorated with antibodies to epidermal growth factor receptors (EGFR) specific to head and neck squamous carcinoma cells (HNSCC), the nano-constructs selectively accumulated in HNSCC tumors in mice. Accumulation of the targeted nanoparticles was observed using two-photon intravital imaging. Furthermore, significant regression of tumor growth was observed in mice treated with the targeted therapeutic hybrid nanotubes. Recently, both MRI-active nanoparticles and quantum dots have been incorporated into the carbon nanotube, and multimodal cellular imaging has been $demonstrated. ^{[279,280]} \\$

Carbon nanotubes have been plated with gold for high-contrast photoacoustic and photothermal imaging by Kim and co-workers. [281] The gold-coated single-walled carbon nanotubes displayed strong plasmonic resonances in the NIR spectrum. When decorated with biomolecules specific

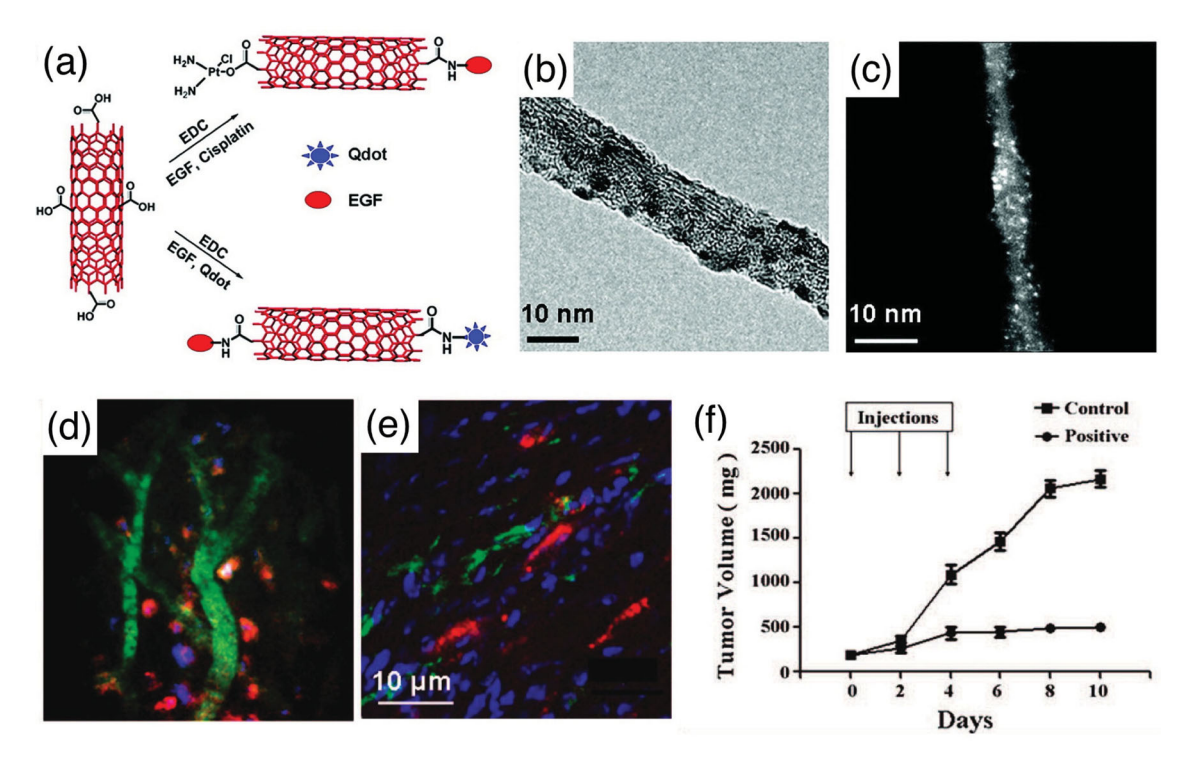


Figure 9. a) Schematic of the fabrication of hybrid nanoparticles based on a carbon nanotube carrier. b) Transmission electron microscope (TEM) image of nanotubes with attached fluorescent quantum dots. c) STEM image of fluorescent nanotube-based drug delivery system. The bright spots are the anti-cancer drug cisplatin. d) Intravital two-photon microscope image of HN12 xenograft tumor. The nanotubes are red, cell nuclei are blue, and blood vessels are green. e) Corresponding confocal microscope images of a tumor slice. f) The fluorescent nanotube-based delivery system shows significant suppression of tumor growth in a mouse model containing HN12 HNSCC xenograft tumors. The theranostic nanotubes were injected intravenously into the mice at 0, 2, and 4 days as indicated. Reproduced with permission from ref.^[278] Copyright © 2009 American Chemical Society.

Adv. Mater. 2012,

LS ______Naryieus

www.MaterialsViews.com

to lymphatic endothelial receptors, the gold-nanotube hybrids could target lymphatic vessels in a live animal, and targeting was imaged non-invasively with an integrated photoacoustic/photothermal technique. The same researchers also demonstrated enrichment of targeted nanoparticles in circulating tumor cells (CTC) in the bloodstream of mice when a CTC-targeting moiety was attached to the nanoparticles.^[282] Carbon nanotubes were also decorated with gold nanocrystals and aptamers for targeted SERS imaging and photothermal therapy of cancer cells.^[283]

Although carbon-based nanotubes are perhaps the most familiar nanotube formulation used in biomedical studies today. silica-based nanotubes are an interesting alternative because of their degradability in biological media. Silica nanotubes can be fabricated by template synthesis using a porous alumina template combined with sol-gel chemistry, and precise control of inner and outer diameters and nanotube lengths has been achieved. [284-286] Importantly, the synthetic procedure provides a means to differentially functionalize the inner and outer surfaces; the interior of the hollow tubular nanostructure can be filled with therapeutic agents, thus protecting them from enzymatic degradation, and the outer surface of the nanostructure can be functionalized with targeting moieties. Additionally, as with the mesoporous silica nanoparticles mentioned earlier, the open ends of silica nanotubes can be chemically gated to control drug release. [287,288] Lee and co-workers developed a magnetic variant by incorporating magnetite nanoparticles on the inner surface of the silica nanotube. [289] The inner voids of these magnetic hybrid nanotubes were able to collect biochemicals, which could then be guided with a magnet. Furthermore, the functionalized exterior facilitated biological interaction between the nanotubes and specific target sites, allowing for more efficient delivery of drugs. The magnetic hybrid nanotubes could be also used as MRI contrast agents.[290]

3. Requirements for Clinical Applications

Although considerable advances have been made in developing hybrid nanoparticles for combined diagnostic and therapeutic, or theranostic, applications in the past decades, there remain significant barriers to their clinical translation. As can be seen in Table 1, which summarizes the recent advances with hybrid nanoparticles, only a few hybrid nanoparticle systems can simultaneously detect and treat malignant tissues in vivo. In contrast to in vitro experiments, once nanoparticles enter into the dynamic bloodstream, they meet and interact with numerous proteins, cells, and tissue surfaces before reaching their intended target site (such as the cancerous tissues). During in vivo circulation, a significant quantity of nanoparticles are non-specfically cleared from the blood by the mononuclear phagocytic system (MPS) in the body—the liver, spleen, and lymph nodes—and the efficiency of this process depends on nanoparticle size and surface chemistry. Thus, hybrid nanoparticles composed of multiple nanocomponents must be engineered to exhibit a long residence time in the bloodstream if systemic administration is to be effective.

To summarize the most important factors determining in vivo behavior of hybrid nanosystems: First, a nanodevice

containing multiple nanomaterial components will naturally be larger than an individual one-component nanoparticle. The size of a nanoparticle is closely tied to in vivo behaviors such as circulation time, circulation rate, extravasation, immunogenicity, degradation, clearance, and cellular internalization. [291] In general, the blood circulation time of a nanoparticle decreases with increasing size, [292] and long-circulating nanoparticles in the size range of 20-100 nm tend to accumulate preferentially at tumor sites via the EPR effect.^[293,294] Thus many hybrid nanosystems tend to be designed and constructed to fall into the 20-100 nm size range. This size range is also the break-even point for payload capacity for hollow (volume-loaded) vs solid (surface-loaded) nanostructures (Figure 1 and Table 1). A PEG coating generally prolongs circulation times of nanoparticles, and it is more effective with the larger nanoparticles.

Second, the mechanical flexibility of a hybrid nanoparticle exerts a large influence on its properties. Hybrids based on flexible nanostructures such as liposomes, micelles, and carbon nanotubes behave differently *in vivo* relative to those built with more rigid nanostructures such as magnetic nanoparticles, gold nanoparticles, and porous silica nanoparticles. Flexibility influences the engagement with cellular surfaces and it may enhance effusional processes. Additionally, flexible nanostructures can be more permeable and they will hold and release a drug payload differently than rigid nanostructures.

Third, hybrid nanoparticles are composed of multiple functional components that all must work in concert to achieve the desired theranostic outcome. Fabricated using many chemical and physical processing steps such as chemical conjugation, electrostatic and hydrophobic condensation, controlled precipitation, and magnetic separation, the more complicated nanostructure of a hybrid nanoparticle may be dissociated into its sub-constituents before accomplishing its intended functions. For example, if an imaging component is stripped from the hybrid nanoparticle during circulation, the biodistribution of the hybrid will not be reported properly and this could lead to a false positive or (more likely) a false negative diagnosis. In addition, the various chemical and nanocrystal components of a hybrid nanoparticle could lead to unintended acute or longterm toxicity if the hybrid goes awry. Thus, careful selection of nanocomponents and chemical agents is required to fabricate reliable and biocompatible hybrid nanoparticles, and considerable attention must be given to the design and in vivo behavior of hybrid nanostructures.

Lastly, incorporation of imaging nanocomponents into a hybrid nanodevice will interfere with the loading of therapeutic agents. Because any nano-superstructure will exhibit toxicity or other undesirable side effects at sufficiently high doses, efficient loading of the drug into a therapeutic nanoparticle is critically important. A co-loaded imaging component must share the limited space or volume available in the hybrid. A hollow hybrid, where the drugs are encapsulated in the interior and the reporting components are decorated on the exterior, is one possibility to maximize each function. Thus, the dual functions to image and to treat the disease could be more synergistically performed with the proper design of a hybrid nano-theranostic.



www.advmat.de

4. Conclusions and Future Prospects

Significant improvements in the synthesis and functionalization of hybrid nanoparticles have been realized in recent years, offering hope for their successful clinical translation. A key promise of these more complicated nanoparticle systems is their demonstrated ability to perform multiple functions in biological systems, and many examples were highlighted in this article. Even single-component nanoparticle formulations perform tasks in vivo that are not achievable with simple imaging or therapeutic molecules. For example, the pharmacokinetics of many therapeutic molecules are significantly improved when incorporated into a nanoparticle formulation, and this has been well demonstrated in the clinic by a few high-profile nanoparticle drugs like Abraxane and Doxil. The unique physicochemical characteristics of nanoparticles have also enabled ultrasensitve in vivo imaging, such as in the clinically approved iron oxide nanoparticle formulation Feridex®. If the more complicated properties of hybrids can be tamed, the combining of such functions into a hybrid nanosystem promises to yield even greater improvements in patient outcomes.

An important pairing of functions that such hybrid nanoparticles can achieve is the simultaneous detection and treatment of a disease, particularly cancer. Theranostic hybrid nanoparticles would allow the clinician to more effectively monitor the progress of cancer and the efficacy of the treatment. As discussed in this article, numerous hybrid nanostructures have been developed to achieve such dual functions in vitro and in vivo. Although some of them are approaching clinical applications, there are many technical and regulatory hurdles to be surmounted before such nanotools become commonplace in the treatment of cancer. Much more effort should be focused on the in vivo behavior of hybrid nanoparticles. Additionally, reliable and reproducible synthetic procedures need to be developed, and their scaling to production levels must be validated. The field needs effective participation and collaboration between chemists, materials scientists, biologists, engineers and clinicians.

Acknowledgements

This work was supported by the Converging Research Center Program of the Ministry of Education, Science and Technology, Korea (Grant No. 2011K000864), the National Cancer Institute of the National Institutes of Health (NIH BRP Grant No. R01CA124427-01) and the National Science Foundation, USA (DMR-0806859).

Received: February 15, 2012 Revised: April 5, 2012 Published online:

- [1] I. Asimov, H. Kleiner, O. Klement, *Fantastic Voyage*, Houghton Mifflin, Boston **1966**.
- [2] M. Ferrari, Nat. Rev. Cancer 2005, 5, 161.
- [3] D. Peer, J. M. Karp, S. Hong, O. C. farokhzad, R. Margalit, R. Langer, Nat. Nanotechnol. 2007, 2, 751.
- [4] M. E. Davis, Z. Chen, D. M. Shin, Nat. Rev. Drug Discov. 2008, 7, 771.

- [5] R. Weissleder, A. Bogdanov, E. A. Neuwelt, M. Papisov, Adv. Drug Deliv. Rev. 1995, 16, 321.
- [6] J. H. Lee, Y. M. Huh, Y. Jun, J. Seo, J. Jang, H. T. Song, S. Kim, E. J. Cho, H. G. Yoon, J. S. Suh, J. Cheon, Nat. Med. 2007, 13, 95.
- [7] J.-H. Park, G. v. Maltzahn, L. Zhang, M. P. Schwartz, E. Ruoslahti, S. N. Bhatia, M. J. Sailor, Adv. Mater. 2008, 20, 1630.
- [8] M. E. Akerman, W. C. W. Chan, P. Laakkonen, S. N. Bhatia, E. Ruoslahti, Proc. Natl Acad. Sci. USA 2002, 99, 12617.
- [9] X. H. Gao, Y. Y. Cui, R. M. Levenson, L. W. K. Chung, S. M. Nie, Nat. Biotechnol. 2004, 22, 969.
- [10] V. P. Torchilin, Mol. Med. Today 1996, 2, 242.
- [11] V. P. Torchilin, Nat. Rev. Drug Discov. 2005, 4, 145.
- [12] I. I. Slowing, B. G. Trewyn, S. Giri, V. S. Y. Lin, Adv. Funct. Mater. 2007, 17, 1225.
- [13] B. G. Trewyn, Slowing II, S. Giri, H. T. Chen, V. S. Y. Lin, Acc. Chem. Res. 2007, 40, 846.
- [14] L. R. Hirsch, R. J. Stafford, J. A. Bankson, S. R. Sershen, B. Rivera, R. E. Price, J. D. Hazle, N. J. Halas, J. L. West, *Proc. Natl Acad. Sci.* USA 2003, 100, 13549.
- [15] X. Huang, I. H. El-Sayed, W. Qian, M. A. El-Sayed, J. Am. Chem. Soc. 2006, 128, 2115.
- [16] Y. Piao, A. Burns, J. Kim, U. Wiesner, T. Hyeon, Adv. Funct. Mater. 2008, 18, 3745.
- [17] J. Cheon, J.-H. Lee, Acc. Chem. Res. 2008, 41, 1630.
- [18] J. Kim, S. Park, J. E. Lee, S. M. Jin, J. H. Lee, I. S. Lee, I. Yang, J.-S. Kim, S. K. Kim, M.-H. Cho, T. Hyeon, Angew. Chem.Int. Ed. 2006, 45, 7754.
- [19] J.-H. Park, G. von Maltzahn, E. Ruoslahti, S. N. Bhatia, M. J. Sailor, Angew. Chem. Int. Ed. 2008, 47, 7284.
- [20] J. Kim, H. S. Kim, N. Lee, T. Kim, H. Kim, T. Yu, I. C. Song, W. K. Moon, T. Hyeon, Angew. Chem. Int. Ed. 2008, 47, 8438.
- [21] A. Bromley, Theranostics: the influence of diagnostics on pharmaceutical therapy, P. J. B. Publications, Richmond, GB 2000.
- [22] A. C. Antony, Blood 1992, 79, 2807.
- [23] S. D. Weitman, R. H. Lark, L. R. Coney, D. W. Fort, V. Frasca, V. R. Zurawski, B. A. Kamen, *Cancer Res.* 1992, 52, 3396.
- [24] H. Zeng, S. Sun, Adv. Funct. Mater. 2007, 18, 391.
- [25] S. A. Corr, Y. P. Rakovich, Y. K. Gun'ko, Nanoscale Res. Lett. 2008, 3,
- [26] R. W. Storrs, F. D. Tropper, H. Y. Li, C. K. Song, J. K. Kuniyoshi, D. A. Sipkins, K. C. P. Li, M. D. Bednarski, J. Am. Chem. Soc. 1995, 117, 7301.
- [27] D. A. Sipkins, D. A. Cheresh, M. R. Kazemi, L. M. Nevin, M. D. Bednarski, K. C. P. Li, *Nat. Med.* **1998**, *4*, 623.
- [28] G. H. Wu, A. Milkhailovsky, H. A. Khant, C. Fu, W. Chiu, J. A. Zasadzinski, J. Am. Chem. Soc. 2008, 130, 8175.
- [29] D. B. Chithrani, M. Dunne, J. Stewart, C. Allen, D. A. Jaffray, Nanomedicine 2010, 6, 161.
- [30] D. Pornpattananangkul, S. Olson, S. Aryal, M. Sartor, C.-M. Huang, K. Vecchio, L. Zhang, ACS Nano 2010, 4, 1935.
- [31] W. T. Al-Jamal, K. T. Al-Jamal, B. Tian, L. Lacerda, P. H. Bomans, P. M. Frederik, K. Kostarelos, ACS Nano 2008, 2, 408.
- [32] S.-H. Park, S.-G. Oh, J.-Y. Mun, S.-S. Han, Colloids Surf. B: Biointerf. 2006, 48, 112.
- [33] M. R. Rasch, E. Rossinyol, J. L. Hueso, B. W. Goodfellow, J. Arbiol, B. A. Korgel, *Nano Lett.* **2010**, *10*, 3733.
- [34] L. Paasonen, T. Sipilä, A. Subrizi, P. Laurinmäki, S. J. Butcher, M. Rappolt, A. Yaghmur, A. Urtti, M. Yliperttula, J. Controlled Release 2010, 147, 136.
- [35] H. Ba, J. Rodriguez-Fernandez, F. D. Stefani, J. Feldmann, *Nano Lett.* 2010, 10, 3006.
- [36] B. Radt, T. A. Smith, F. Caruso, Adv. Mater. 2004, 16, 2184.
- [37] A. G. Skirtach, C. Dejugnat, D. Braun, A. S. Susha, A. L. Rogach, W. J. Parak, H. Mohwald, G. B. Sukhorukov, Nano Lett. 2005, 5, 1371.



www.MaterialsViews.com

- [38] L. Paasonen, T. Laaksonen, C. Johans, M. Yliperttula, K. Kontturi, A. Urtti, J. Controlled Release 2007, 122, 86.
- [39] D. V. Volodkin, A. G. Skirtach, H. Mohwald, Angew. Chem. Int. Ed. 2009, 48, 1807.
- [40] S. Lesieur, C. Grabielle-Madelmont, C. Menager, V. Cabuil, D. Dadhi, P. Pierrot, K. Edwards, J. Am. Chem. Soc. 2003, 125, 5266.
- [41] M.-S. Martina, J.-P. Fortin, C. Menager, O. Clement, G. Barratt, C. Grabielle-Madelmont, F. Gazeau, V. Cabuil, S. Lesieur, J. Am. Chem. Soc. 2005, 127, 10676.
- [42] T.-Y. Liu, T. C. Huang, Acta Biomater. 2011, 7, 3927.
- [43] Y. Chen, A. Bose, G. D. Bothun, ACS Nano 2010, 4, 3215.
- [44] G. Mikhaylov, UrsaMikac, A. A. Magaeva, V. I. Itin, E. P. Naiden, I. Psakhye, L. Babes, T. Reinheckel, C. Peters, R. Zeiser, M. Bogyo, V. Turk, S. G. Psakhye, B. Turk, O. Vasiljeva, *Nat. Nanotechnol.* 2011, 6, 594.
- [45] J. M. Perez, L. Josephson, T. O'Loughlin, D. Högemann, R. Weissleder, Nat. Biotechnol. 2002, 20, 816.
- [46] M. Shinkai, M. Yanase, H. Honda, T. Wakabayashi, J. Yoshida, T. Kobayashi, Cancer Sci. 1996, 87, 1179.
- [47] A. Ito, K. Tanaka, K. Kondo, M. Shinkai, H. Honda, K. Matsumoto, T. Saida, T. Kobayashi, *Cancer Sci.* 2003, 94, 308.
- [48] L.-A. Tai, P.-J. Tsai, Y.-C. Wang, Y.-J. Wang, L.-W. Lo, C.-S. Yang, Nanotechnology 2009, 20, 135101.
- [49] J.-P. Fortin-Ripoche, M. S. Martina, F. Gazeau, C. Menager, C. Wilhelm, J.-C. Bacri, S. Lesieur, O. Clement, *Radiology* 2006, 239, 415.
- [50] G. D. Bothun, A. E. Rabideau, M. A. Stoner, J. Phys. Chem. B 2009, 113, 7725.
- [51] V. Sigot, D. J. Arndt-Jovin, T. M. Jovin, Bioconjugate Chem. 2010, 21, 1465.
- [52] J. Pan, D. Wan, J. Gong, Chem. Commun. 2011, 47, 3442.
- [53] W. T. Al-Jamal, K. T. Al-Jamal, P. H. Bomans, P. M. Frederik, K. Kostarelos, *Small* **2008**, *4*, 1406.
- [54] B. Tian, W. T. Al-Jamal, K. T. Al-Jamal, K. Kostarelos, Int. J. Pharm. 2011, 416, 443.
- [55] G. Gopalakrishnan, C. Danelon, P. Izewska, M. Prummer, P.-Y. Bolinger, I. Geissbuhler, D. Demurtas, J. Dubochet, H. Vogel, Angew. Chem. Int. Ed. 2006, 45, 5478.
- [56] W. T. Al-Jamal, K. T. Al-Jamal, B. Tian, A. Cakebread, J. M. Halke, K. Kostarelos, Mol. Pharmaceutics 2009, 6, 520.
- [57] G. Beaune, B. Dubertret, O. Clement, C. Vayssettes, V. Cabuil, C. Menager, Angew. Chem. Int. Ed. 2007, 46, 5421.
- [58] H. Nobuto, T. Sugita, T. Kubo, S. Shimose, Y. Yasunaga, T. Murakami, M. Ochi, Int. J. Cancer 2004, 109, 627.
- [59] K. C. Weng, C. O. Noble, B. Papahadjopoulos-Sternberg, F. F. Chen, D. C. Drummond, D. B. Kirpotin, D. H. Wang, Y. K. Hom, B. Hann, J. W. Park, *Nano Lett.* 2008, 8, 2851.
- [60] V. P. Torchilin, A. N. Lukyanov, Z. Gao, B. Papahadjopoulos-Sternberg, Proc. Natl Acad. Sci. USA 2003, 100, 6039.
- [61] R. Savic, L. B. Luo, A. Eisenberg, D. Maysinger, Science 2003, 300, 615.
- [62] V. P. Torchilin, Pharm. Res. 2007, 24, 1.
- [63] Z. Gao, A. N. Lukyanov, A. Singhal, V. P. Torchilin, Nano Lett. 2002, 2 979
- [64] N. Nasongkla, X. Shuai, H. Ai, B. D. Weinberg, J. Pink, D. A. Boothman, J. Gao, Angew. Chem. Int. Ed. 2004, 43, 6323.
- [65] M. R. Kano, Y. Bae, C. Iwata, Y. Morishita, M. Yashiro, M. Oka, T. Fujii, A. Komuro, K. Kiyono, M. Kaminishi, K. Hirakawa, Y. Ouchi, N. Nishiyama, K. Kataoka, K. Miyazono, *Proc. Natl Acad. Sci. USA* 2007, 104, 3460.
- [66] Y. Geng, P. Dalhaimer, S. Cai, R. Tsai, M. Tewari, T. Minko, D. E. Discher, Nat. Nanotechnol. 2007, 2, 249.

- [67] M. Murakami, H. Cabral, Y. Matsumoto, S. Wu, M. R. Kano, T. Yamori, N. Nishiyama, K. Kataoka, Sci. Trans. Med. 2011, 3, 64ra?
- [68] H. Cabral, Y. Matsumoto, K. Mizuno, Q. Chen, M. Murakami, M. Kimura, Y. Terada, M. R. Kano, K. Miyazono, M. Uesaka, N. Nishiyama, K. Kataoka, Nat. Nanotechnol. 2011, 6, 815.
- [69] I. L. Medintz, H. T. Uyeda, E. R. Goldman, H. Mattoussi, *Nature Mater.* 2005, 4, 435.
- [70] X. Michalet, F. F. Pinaud, L. A. Bentolila, J. M. Tsay, S. Doose, J. J. Li, G. Sundaresan, A. M. Wu, S. S. Gambhir, S. Weiss, *Science* 2005, 307, 538.
- [71] J. Park, E. Lee, N. M. Hwang, M. S. Kang, S. C. Kim, Y. Hwang, J. G. Park, H. J. Noh, J. Y. Kini, J. H. Park, T. Hyeon, *Angew. Chem. Int. Ed.* 2005, 44, 2872.
- [72] J. Park, J. Joo, S. G. Kwon, Y. Jang, T. Hyeon, Angew. Chem. Int. Ed. 2007, 46, 4630.
- [73] S. G. Kwon, T. Hyeon, Accounts of Chemical Research 2008, 41, 1696.
- [74] M. Bruchez, M. Moronne, P. Gin, S. Weiss, A. P. Alivisatos, *Science* 1998, 281, 2013.
- [75] W. C. W. Chan, S. Nie, Science 1998, 281, 2016.
- [76] B. Dubertret, P. Skourides, D. J. Norris, V. Noireaux, A. H. Brivanlou, A. Libchaber, *Science* 2002, 298, 1759.
- [77] G. A. F. van Tilborg, W. J. M. Mulder, P. T. K. Chin, G. Storm, C. P. Reutelingsperger, K. Nicolay, G. J. Strijkers, *Bioconjugate Chem.* 2006, 17, 865.
- [78] B. S. Kim, J. M. Qiu, J. P. Wang, T. A. Taton, Nano Lett. 2005, 5, 1987.
- [79] H. Ai, C. Flask, B. Weinberg, X. Shuai, M. D. Pagel, D. Farrell, J. Duerk, J. M. Gao, Adv. Mater. 2005, 17, 1949.
- [80] D. R. Larson, W. R. Zipfel, R. M. Williams, S. W. Clark, M. P. Bruchez, F. W. Wise, W. W. Webb, *Science* 2003, 300, 1434.
- [81] X. Y. Wu, H. J. Liu, J. Q. Liu, K. N. Haley, J. A. Treadway, J. P. Larson, N. F. Ge, F. Peale, M. P. Bruchez, Nat. Biotechnol. 2003, 21, 41.
- [82] B. Ballou, B. C. Lagerholm, L. A. Ernst, M. P. Bruchez, A. S. Waggoner, Bioconjugate Chem. 2004, 15, 79.
- [83] W. S. Seo, J. H. Lee, X. M. Sun, Y. Suzuki, D. Mann, Z. Liu, M. Terashima, P. C. Yang, M. V. McConnell, D. G. Nishimura, H. J. Dai, Nat. Mater. 2006, 5, 971.
- [84] H. B. Na, J. H. Lee, K. J. An, Y. I. Park, M. Park, I. S. Lee, D. H. Nam, S. T. Kim, S. H. Kim, S. W. Kim, K. H. Lim, K. S. Kim, S. O. Kim, T. Hyeon, Angew. Chem. Int. Ed. 2007, 46, 5397.
- [85] G. A. F. van Tilborg, W. J. M. Mulder, N. Deckers, G. Storm, C. P. M. Reutelingsperger, G. J. Strijkers, K. Nicolay, *Bioconjugate Chem.* 2006, 17, 741.
- [86] W. J. M. Mulder, R. Koole, R. J. Brandwijk, G. Storm, P. T. K. Chin, G. J. Strijkers, C. D. Donega, K. Nicolay, A. W. Griffioen, *Nano Lett.* 2006, 6, 1.
- [87] B.-S. Kim, T. A. Taton, Langmuir 2007, 23, 2198.
- [88] F. Erogbogbo, K.-T. Yong, R. Hu, W.-C. Law, H. Ding, C.-W. Chang, P. N. Prasad, M. T. Swihart, ACS Nano 2010, 9, 5131.
- [89] X. Yang, J. J. Grailer, I. J. Rowland, A. Javadi, S. A. Hurley, D. A. Steeber, S. Gong, Biomaterials 2010, 31, 9065.
- [90] C. Liao, Q. Sun, B. Liang, J. Shen, X. Shuai, Eur. J. Radiol. 2011, 80, 699.
- [91] J. Hu, Y. Qian, X. Wang, T. Liu, S. Liu, Langmuir 2012, 28, 2073.
- [92] T. K. Jain, M. A. Morales, S. K. Sahoo, D. L. Leslie-Pelecky, V. Labhasetwar, Mol. Pharmaceutics 2005, 2, 194.
- [93] T. K. Jain, J. Richey, M. Strand, D. L. Leslie-Pelecky, C. A. Flask, V. Labhasetwar, *Biomaterials* 2008, 29, 4012.
- [94] L. O. Cinteza, T. Y. Ohulchanskyy, Y. Sahoo, E. J. Bergey, R. K. Pandey, P. N. Prasad, Mol. Pharmaceutics 2006, 3, 415.
- [95] P. Zou, Y. Yu, Y. A. Wang, Y. Zhong, A. Welton, C. Galban, S. Wang, D. Sun, Mol. Pharmaceutics 2010, 6, 1974.

www.advmat.de

www.MaterialsViews.com

- [96] W. Wang, D. Cheng, F. Gong, X. Miao, X. Shuai, Adv. Mater. 2012, 24, 115.
- [97] N. Nasongkla, E. Bey, J. Ren, H. Ai, C. Khemtong, J. S. Guthi, S.-F. Chin, A. D. Sherry, D. A. Boothman, J. Gao, *Nano Lett.* 2006, 6, 2427.
- [98] J. S. Guthi, S.-G. Yang, G. Huang, S. Li, C. Khemtong, C. W. Kessinger, M. Peyton, J. D. Minna, K. C. Brown, J. Gao, Mol. Pharmaceutics 2009, 7, 32.
- [99] Y. Namiki, T. Namiki, H. Yoshida, Y. Ishii, A. Tsubota, S. Koido, K. Nariai, M. Mitsunaga, S. Yanagisawa, H. Kashiwagi, Y. Mabashi, Y. Yumoto, S. Hoshina, K. Fujise, N. Tada, *Nat. Nanotechnol.* 2009, 4, 598.
- [100] G. H. Gao, G. H. Im, M. S. Kim, J. W. Lee, J. Yang, H. Jeon, J. H. Lee, D. S. Lee, Small 2010, 11, 1201.
- [101] D. Chen, X. Xia, H. Gu, Q. Xu, J. Ge, Y. Li, N. Li, J. Lu, J. Mater. Chem. 2011, 21, 12682.
- [102] H. Xu, L. Cheng, C. Wang, X. Ma, Y. Li, Z. Liu, Biomaterials 2011, 32, 9364.
- [103] S. Sengupta, D. Eavarone, I. Capila, G. L. Zhao, N. Watson, T. Kiziltepe, R. Sasisekharan, *Nature* 2005, 436, 568.
- [104] Slowing, II, J. L. Vivero-Escoto, C. W. Wu, V. S. Y. Lin, Adv. Drug Deliv. Rev. 2008, 60, 1278.
- [105] D. R. Radu, C. Y. Lai, K. Jeftinija, E. W. Rowe, S. Jeftinija, V. S. Y. Lin, J. Am. Chem. Soc. 2004, 126, 13216.
- [106] I. Slowing, B. G. Trewyn, V. S. Y. Lin, J. Am. Chem. Soc. 2006, 128, 14792
- [107] H. Vallhov, S. Gabrielsson, M. Stromme, A. Scheynius, A. E. Garcia-Bennett, *Nano Lett.* 2007, 7, 3576.
- [108] C. Y. Lai, B. G. Trewyn, D. M. Jeftinija, K. Jeftinija, S. Xu, S. Jeftinija, V. S. Y. Lin, J. Am. Chem. Soc. 2003, 125, 4451.
- [109] S. Giri, B. G. Trewyn, M. P. Stellmaker, V. S. Y. Lin, Angew. Chem. Int. Ed. 2005, 44, 5038.
- [110] J. K. Hsiao, C. P. Tsai, T. H. Chung, Y. Hung, M. Yao, H. M. Liu, C. Y. Mou, C. S. Yang, Y. C. Chen, D. M. Huang, *Small* **2008**, *4*, 1445
- [111] S. H. Wu, Y. S. Lin, Y. Hung, Y. H. Chou, Y. H. Hsu, C. Chang, C. Y. Mou, Chembiochem 2008, 9, 53.
- [112] Y.-S. Lin, Y. Hung, J.-K. Su, R. Lee, C. Chang, M.-L. Lin, C.-Y. Mou, J. Phys. Chem. B 2004, 108, 15608.
- [113] Y.-S. Lin, C.-P. Tsai, H.-Y. Huang, C.-T. Kuo, Y. Hung, D.-M. Huang, Y.-C. Chen, C.-Y. Mou, Chem. Mater. 2005, 17, 4570.
- [114] M. Benezra, O. Penate-Medina, P. B. Zanzonico, D. Schaer, H. Ow, A. Burns, E. DeStanchina, V. Longo, E. Herz, S. Iyer, J. Wolchok, S. M. Larson, U. Wiesner, M. S. Bradbury, J. Clin. Invest. 2011, 121, 2768.
- [115] F. Torney, B. G. Trewyn, V. S. Y. Lin, K. Wang, Nat. Nanotechnol. 2007, 2, 295.
- [116] C. H. Lee, L. W. Lo, C. Y. Mou, C. S. Yang, Adv. Funct. Mater. 2008, 18, 3283.
- [117] W. Cai, I. R. Gentle, G. Q. Lu, J.-J. Zhu, A. Yu, Anal. Chem. 2008, 80, 5401.
- [118] C.-H. Lee, S.-H. Cheng, I.-P. Huang, J. S. Souris, C.-S. Yang, C.-Y. Mou, L.-W. Lo, Angew. Chem. Int. Ed. 2010, 49, 8214
- [119] C. R. Thomas, D. P. Ferris, J.-H. Lee, E. Choi, M. H. Cho, E. S. Kim, J. F. Stoddart, J.-S. Shin, J. Cheon, J. I. Zink, J. Am. Chem. Soc. 2010, 132, 10623.
- [120] P. Wu, J. Zhu, Z. Xu, Adv. Funct. Mater. 2004, 14, 345.
- [121] W. Zhao, J. Gu, L. Zhang, H. Chen, J. Shi, J. Am. Chem. Soc. 2005, 127, 8916
- [122] J. Lee, Y. Lee, J. K. Youn, H. Bin Na, T. Yu, H. Kim, S. M. Lee, Y. M. Koo, J. H. Kwak, H. G. Park, H. N. Chang, M. Hwang, J. G. Park, J. Kim, T. Hyeon, *Small* **2008**, *4*, 143.
- [123] M. Liong, J. Lu, M. Kovochich, T. Xia, S. G. Ruehm, A. E. Nel, F. Tamanoi, J. I. Zink, ACS Nano 2008, 2, 889.

- [124] T. Sen, A. Sebastianelli, I. J. Bruce, J. Am. Chem. Soc. 2006, 128, 7130.
- [125] F.-H. Chen, L.-M. Zhang, Q.-T. Chen, Y. Zhang, Z.-J. Zhang, Chem. Commun. 2010, 46, 8633.
- [126] B. Chang, J. Guo, C. Liu, J. Qian, W. Yang, J. Mater. Chem. 2010, 20, 9941
- [127] D. Chen, M. Jiang, N. Li, H. Gu, Q. Xu, J. Ge, X. Xia, J. Lu, J. Mater. Chem. 2010, 20, 6422.
- [128] J. Kim, J. E. Lee, J. Lee, J. H. Yu, B. C. Kim, K. An, Y. Hwang, C.-H. Shin, J.-G. Park, J. Kim, T. Hyeon, J. Am. Chem. Soc. 2005, 128, 688.
- [129] Y. Chen, H. Chen, S. Zhang, F. Chen, L. Zhang, J. Zhang, M. Zhu, H. Wu, L. Guo, J. Feng, J. Shi, Adv. Funct. Mater. 2011, 21, 270.
- [130] I. Gorelikov, N. Matsuura, Nano Lett. 2008, 8, 369.
- [131] Q. Zhan, J. Qian, X. Li, S. He, Nanotechnology 2010, 21, 055704.
- [132] T. Zhao, H. Wu, S. Q. Yao, Q.-H. Xu, G. Q. Xu, Langmuir 2010, 26, 14937.
- [133] H. S. Qian, H. C. Guo, P. C.-L. Ho, R. Mahendran, Y. Zhang, Small 2009, 5, 2285.
- [134] J. E. Lee, N. Lee, H. Kim, J. Kim, S. H. Choi, J. H. Kim, T. Kim, I. C. Song, S. P. Park, W. K. Moon, T. Hyeon, J. Am. Chem. Soc. 2009, 132, 552.
- [135] J. E. Lee, D. J. Lee, N. Lee, B. H. Kim, S. H. Choi, T. Hyeon, J. Mater. Chem. 2011, 21, 16869.
- [136] J. Liu, A. Stace-Naughton, X. Jiang, C. J. Brinker, J. Am. Chem. Soc. 2009, 131, 1354.
- [137] C. E. Ashley, E. C. Carnes, G. K. Phillips, D. Padilla, P. N. Durfee, P. A. Brown, T. N. Hanna, J. Liu, B. Phillips, M. B. Carter, N. J. Carroll, X. Jiang, D. R. Dunphy, C. L. Willman, D. N. Petsev, D. G. Evans, A. N. Parikh, B. Chackerian, W. Wharton, D. S. Peabody, C. J. Brinker, *Nature Mater.* 2011, 10, 389.
- [138] L. Li, F. Tang, H. Liu, T. Liu, N. Hao, D. Chen, X. Teng, J. He, ACS Nano 2010. 4, 6874.
- [139] Y. Hu, X. T. Zheng, J. S. Chen, M. Zhou, C. M. Li, X. W. D. Lou, J. Mater. Chem. 2011, 21, 8052.
- [140] L. Li, Y. Guan, H. Liu, N. Hao, T. Liu, X. Meng, C. Fu, Y. Li, Q. Qu, Y. Zhang, S. Ji, L. Chen, D. Chen, F. Tang, ACS Nano 2011, 9, 7462.
- [141] H. Liu, D. Chen, L. Li, T. Liu, L. Tan, X. Wu, F. Tang, Angew. Chem. Int. Ed. 2010, 50, 891.
- [142] F. Zhang, G. B. Braun, A. Pallaoro, Y. Zhang, Y. Shi, D. Cui, M. Moskovits, D. Zhao, G. D. Stucky, Nano Lett. 2011, 12, 61.
- [143] H. S. Yoo, J. E. Oh, K. H. Lee, T. G. Park, Pharm. Res. 1999, 16, 1114.
- [144] H. S. Yoo, K. H. Lee, J. E. Oh, T. G. Park, J. Controlled Release 2000, 68, 419.
- [145] K. S. Soppimath, T. M. Aminabhavi, A. R. Kulkarni, W. E. Rudzinski, J. Controlled Release 2001, 70, 1.
- [146] H. S. Sakhalkar, M. K. Dalal, A. K. Salem, R. Ansari, A. Fu, M. F. Kiani, D. T. Kurjiaka, J. Hanes, K. M. Shakesheff, D. J. Goetz, Proc. Natl Acad. Sci. USA 2003, 100, 15895.
- [147] S. S. Feng, L. Mu, K. Y. Win, G. F. Huang, Curr. Med. Chem. 2004, 11, 413.
- [148] J. R. McCarthy, J. M. Perez, C. Bruckner, R. Weissleder, *Nano Lett.* 2005, 5, 2552.
- [149] F. Gu, L. Zhang, B. A. Teply, N. Mann, A. Wang, A. F. Radovic-Moreno, R. Langer, O. C. Farokhzad, *Proc. Natl Acad. Sci. USA* 2008, 105, 2586.
- [150] S. Dhar, F. X. Gu, R. Langer, O. C. Farokhzad, S. J. Lippard, *Proc. Natl Acad. Sci. USA* 2008, 105, 17356.
- [151] O. C. Farokhzad, J. J. Cheng, B. A. Teply, I. Sherifi, S. Jon, P. W. Kantoff, J. P. Richie, R. Langer, Proc. Natl Acad. Sci. USA 2006, 103, 6315.
- [152] M. Chorny, I. Fishbein, H. D. Danenberg, G. Golomb, J. Controlled Release 2002, 83, 389.

Adv. Mater. 2012,

- [153] C. S. Chaw, Y. Y. Yang, I. J. Lim, T. T. Phan, J. Microencapsulation 2003, 20, 349.
- [154] A. L. Doiron, K. Chu, A. Ali, L. Brannon-Peppas, Proc. Natl Acad. Sci. USA 2008, 105, 17232.
- [155] Y. Wang, Y. W. Ng, Y. Chen, B. Shuter, J. Yi, J. Ding, S. C. Wang, S. S. Feng, Adv. Funct. Mater. 2008, 18, 308.
- [156] X. Q. Liu, M. D. Kaminski, H. T. Chen, M. Torno, L. Taylor, A. J. Rosengart, J. Controlled Release 2007, 119, 52.
- [157] J. Yang, C.-H. Lee, J. Park, S. Seo, E.-K. Lim, Y. J. Song, J.-S. Suh, H.-G. Yoon, Y.-M. Huh, S. Haam, J. Mater. Chem. 2007, 17, 2695.
- [158] S.-B. Seo, J. Yang, W. Hyung, E.-J. Cho, T.-I. Lee, Y. J. Song, H.-G. Yoon, J.-S. Suh, Y.-M. Huh, S. Haam, Nanotechnology 2007, 18, 475105.
- [159] V. Zavisova, M. Koneracka, M. Muckova, P. Kopcansky, N. Tomasovicova, G. Lancz, M. Timko, B. Patoprsta, P. Bartos, M. Fabian, J. Magn. Magn. Mater. 2009, 321, 1613.
- [160] F. Li, J. Sun, H. Zhu, X. Wen, C. Lin, D. Shi, Colloids Surf. B: Biointerf. 2011, 88, 58.
- [161] B. J. Nehilla, P. G. Allen, T. A. Desai, ACS Nano 2008, 2, 538.
- [162] J. Kim, J. E. Lee, S. H. Lee, J. H. Yu, J. H. Lee, T. G. Park, T. Hyeon, Adv. Mater. **2008**, 20, 478.
- [163] N. Andhariya, B. Chudasama, R. V. Mehta, R. V. Upadhyay, J. Nanopart. Res. 2011, 13, 1677.
- [164] H. Park, J. Yang, S. Seo, K. Kim, J. Suh, D. Kim, S. Haam, K. H. Yoo, Small 2008, 4, 192.
- [165] B. S. Zolnik, P. E. Leary, D. J. Burgess, J. Controlled Release 2006, 112, 293.
- [166] H. Park, J. Yang, J. Lee, S. Haam, I.-H. Choi, K.-H. Yoo, ACS Nano 2009, 3, 2919.
- [167] S.-M. Lee, H. Park, K.-H. Yoo, Angew. Chem. Int. Ed. 2010, 22, 4049.
- [168] F.-Y. Cheng, C.-H. Su, P.-C. Wu, C.-S. Yeh, Chem. Comm. 2010, 46, 3167.
- [169] A. Singh, F. Dilnawaz, S. Mewar, U. Sharma, N. R. Jagannathan, S. K. Sahoo, ACS Appl. Mater. Interfaces 2011, 3, 842.
- [170] P.-W. Lee, S.-H. Hsu, J.-S. Tsai, F.-R. Chen, P.-J. Huang, C.-J. Ke, Z.-X. Liao, C.-W. Hsiao, H.-J. Lin, H.-W. Sung, Biomaterials 2010, 31, 2425.
- [171] H.-S. Cho, Z. Dong, G. M. Pauletti, J. Zhang, H. Xu, H. Gu, L. Wang, R. C. Ewing, C. Huth, F. Wang, D. Shi, ACS Nano 2010, 4,
- [172] J. Yang, C. H. Lee, H. J. Ko, J. S. Suh, H. G. Yoon, K. Lee, Y. M. Huh, S. Haam, Angew. Chem. Int. Ed. 2007, 46, 8836.
- [173] T. Yamada, Y. Iwasaki, H. Tada, H. Iwabuki, M. K. Chuah, T. VandenDriessche, H. Fukuda, A. Kondo, M. Ueda, M. Seno, K. Tanizawa, S. Kuroda, Nat. Biotechnol. 2003, 21, 885.
- [174] N. F. Steinmetz, Nanomedicine 2010, 6, 634.
- [175] F. M. Brunel, J. D. Lewis, G. Destito, N. F. Steinmetz, M. Manchester, H. Stuhlmann, P. E. Dawson, Nano Lett. 2010, 10, 1093.
- [176] N. F. Steinmetz, A. L. Ablack, J. L. Hickey, J. Ablack, B. Manocha, J. S. Mymryk, L. G. Luyt, J. D. Lewis, Small 2011, 7, 1664.
- [177] M. L. Flenniken, L. O. Liepold, B. E. Crowley, D. A. Willits, M. J. Young, T. Douglas, Chem. Commun. 2005, 447.
- [178] I. Yacoby, M. Shamis, H. Bar, D. Shabat, I. Benhar, Antimicrob. Agents Chemother. 2006, 50, 2087.
- [179] Y. Ren, S. M. Wong, L.-Y. Lim, Bioconjugate Chem. 2007, 18, 836.
- [180] P. A. Suci, Z. Varpness, E. Gillitzer, T. Douglas, M. Young, Langmuir 2007, 23, 12280.
- [181] H. Bar, I. Yacoby, I. Benhar, BMC Biotechnol. 2008, 8, 37.
- [182] L. Loo, R. H. Guenther, S. A. Lommel, S. Franzen, Chem. Commn.
- [183] J. K. Raty, T. Liimatainen, T. Wirth, K. J. Airenne, T. O. Ihalainen, T. Huhtala, E. Hamerlynck, M. Vihinen-Ranta, A. Narvanen, S. Yla-Herttuala, J. M. Hakumaki, Gene Ther. 2006, 13, 1440.

- [184] A. A. Martinez-Morales, N. G. Portney, Y. Zhang, G. Destito, G. Budak, E. Ozbay, M. Manchester, C. S. Ozkan, M. Ozkan, Adv. Mater. 2008, 20, 1.
- [185] N. Tresilwised, P. Pithayanukul, P. S. Holm, U. Schillinger, C. Plank, O. Mykhaylyk, Biomaterials 2012, 33, 256.
- [186] A. Hofmann, D. Wenzel, U. M. Becher, D. F. Freitag, A. M. Klein, D. Eberbeck, M. Schulte, K. Zimmermann, C. Bergemann, B. Gleich, W. Roell, T. Weyh, L. Trahms, G. Nickenig, B. K. Fleischmann, A. Pfeifer, Proc. Natl Acad. Sci. USA 2009, 106, 44.
- [187] K. Kamei, Y. Mukai, H. Kojima, T. Yoshikawa, M. Yoshikawa, G. Kiyohara, T. A. Yamamoto, Y. Yoshioka, N. Okada, S. Seino, S. Nakagawa, Biomaterials 2009, 30, 1809.
- [188] N. Tresilwised, P. Pithayanukul, O. Mykhaylyk, P. S. Holm, R. Holzmuller, M. Anton, S. Thalhammer, D. Adiguzel, M. Doblinger, C. Plank, Mol. Pharmaceutics 2010, 7, 1069.
- [189] N. G. Portney, K. Singh, S. Chaudhary, G. Destito, A. Schneemann, M. Manchester, M. Ozkan, Langmuir 2005, 21, 2098.
- [190] S. K. Dixit, N. L. Goicochea, M.-C. Daniel, A. Murali, L. Bronstein, M. De, B. Stein, V. M. Rotello, C. C. Kao, B. Dragnea, Nano Lett. **2006**, 6, 1993.
- [191] E. L. Bentzen, F. House, T. J. Utley, Crowe, E. James, D. W. Wright, Nano Lett. 2005, 5, 591.
- [192] F. Li, Z.-P. Zhang, J. Peng, Z.-Q. Cui, D.-W. Pang, K. Li, H.-P. Wei, Y.-F. Zhou, J.-K. Wen, X.-E. Zhang, Small 2009, 5, 718.
- [193] H. Liu, Y. Liu, S. Liu, D.-W. Pang, G. Xiao, J. Virology 2011, 85, 6252.
- [194] C. Chen, M.-C. Daniel, Z. T. Quinkert, M. De, B. Stein, V. D. Bowman, P. R. Chipman, V. M. Rotello, C. C. Kao, B. Dragnea, Nano Lett. 2006, 6, 611.
- [195] X. Huang, L. M. Bronstein, J. Retrum, C. Dufort, I. Tsvetkova, S. Aniagyei, B. Stein, G. Stucky, B. McKenna, N. Remmes, D. Baxter, C. C. Kao, B. Dragnea, Nano Lett. 2007, 7, 2407.
- [196] B. Dragnea, C. Chen, E.-S. Kwak, B. Stein, C. C. Kao, J. Am. Chem. Soc. 2003, 125, 6374.
- [197] T. Wang, Z. Zhang, D. Gao, F. Li, H. Wei, X. Liang, Z. Cui, X.-E. Zhang, Nanoscale 2011, 3, 4275.
- [198] K. Benihoud, P. Yeh, M. Perricaudet, Curr. Opin. Biotechnol. 1999, 10, 440.
- [199] Y.-M. Huh, E.-S. Lee, J.-H. Lee, Y.-w. Jun, P.-H. Kim, C.-O. Yun, J.-H. Kim, J.-S. Suh, J. Cheon, Adv. Mater. 2007, 19, 3109.
- [200] M. Everts, V. Saini, J. L. Leddon, R. J. Kok, M. Stoff-Khalili, M. A. Preuss, C. L. Millican, G. Perkins, J. M. Brown, H. Bagaria, D. E. Nikles, D. T. Johnson, V. P. Zharov, D. T. Curiel, Nano Lett. 2006, 6, 587.
- [201] N. F. Steinmetz, V. Hong, E. D. Spoerke, P. Lu, K. Breitenkamp, M. G. Finn, M. Manchester, J. Am. Chem. Soc. 2009, 131, 17093.
- [202] M. Vieweger, N. Goicochea, E. S. Koh, B. Dragnea, ACS Nano **2011**, 5, 7324.
- [203] H. Yi, D. Ghosh, M.-H. Ham, J. Qi, P. W. Barone, M. S. Strano, A. M. Belcher, NAno Lett. 2012, 12, 1176.
- [204] P. K. Jain, X. Huang, I. H. El-Sayed, M. A. El-Sayed, Acc. Chem. Res. 2008, 41, 1578.
- [205] J. F. Hainfeld, D. N. Slatkin, T. M. Focella, H. M. Smilowitz, Br. J. Radiol. **2006**, 79, 248.
- [206] D. Kim, S. Park, J. H. Lee, Y. Y. Jeong, S. Jon, J. Am. Chem. Soc. 2007, 129, 7661.
- [207] R. Popovtzer, A. Agrawal, N. A. Kotov, A. Popovtzer, J. Balter, T. E. Carey, R. Kopelman, Nano Lett. 2008, 8, 4593.
- [208] C. Xu, G. A. Tung, S. Sun, Chem. Mater. 2008, 20, 4167.
- [209] C. Loo, A. Lowery, N. Halas, J. West, R. Drezek, Nano Lett. 2005, 5,
- [210] I. H. El-Sayed, X. Huang, M. A. El-Sayed, Nano Lett. 2005, 5, 829.
- [211] A. M. Gobin, M. H. Lee, N. J. Halas, W. D. James, R. A. Drezek, J. L. West, Nano Lett. 2007, 7, 1929.



www.advmat.de

www.MaterialsViews.com

- [212] M. C. Skala, M. J. Crow, A. Wax, J. A. Izatt, Nano Lett. 2008, 8, 3461.
- [213] H. F. Wang, T. B. Huff, D. A. Zweifel, W. He, P. S. Low, A. Wei, J. X. Cheng, Proc. Natl Acad. Sci. USA 2005, 102, 15752.
- [214] J. Park, A. Estrada, K. Sharp, K. Sang, J. A. Schwartz, D. K. Smith, C. Coleman, J. D. Payne, B. A. Korgel, A. K. Dunn, J. W. Tunnell, Optics Express 2008, 16, 1590.
- [215] X. Yang, S. E. Skrabalak, Z.-Y. Li, Y. Xia, L. V. Wang, Nano Lett. 2007, 7, 3798.
- [216] K. H. Song, C. Kim, C. M. Cobley, Y. Xia, L. V. Wang, Nano Lett. 2009, 9, 183.
- [217] T. A. Taton, C. A. Mirkin, R. L. Letsinger, Science 2000, 289, 1757.
- [218] J.-M. Nam, C. S. Thaxton, C. A. Mirkin, Science 2003, 301, 1884.
- [219] S. Nie, S. R. Emory, Science 1997, 275, 1102.
- [220] X. Huang, I. H. El-Sayed, W. Qian, M. A. El-Sayed, Nano Lett. 2007, 7, 1591.
- [221] J. Xie, Q. Zhang, J. Y. Lee, D. I. C. Wang, ACS Nano 2008, 2, 2473.
- [222] X. Qian, X.-H. Peng, D. O. Ansari, Q. Yin-Goen, G. Z. Chen, D. M. Shin, L. Yang, A. N. Young, M. D. Wang, S. Nie, *Nat. Biotechnol.* 2008, 26, 83.
- [223] A. S. Thakor, R. Luong, R. Paulmurugan, F. I. Lin, P. Kempen, C. Zavaleta, P. Chu, T. F. Massoud, R. Sinclair, S. S. Gambhir, Sci. Trans. Med. 2011, 3, 79ra33.
- [224] S. E. Skrabalak, J. Chen, Y. Sun, X. Lu, L. Au, C. M. Cobley, Y. Xia, Acc. Chem. Res. 2008, 41, 1587.
- [225] S. Lal, S. E. Clare, N. J. Halas, Acc. Chem. Res. 2008, 41, 1842.
- [226] L. Au, D. Zheng, F. Zhou, Z.-Y. Li, X. Li, Y. Xia, ACS Nano 2008, 2, 1645.
- [227] T. S. Hauck, T. L. Jennings, T. Yatsenko, J. C. Kumaradas, W. C. W. Chan, Adv. Mater. 2008, 20, 3832.
- [228] P. Diagaradjane, A. Shetty, J. C. Wang, A. M. Elliott, J. Schwartz, S. Shentu, H. C. Park, A. Deorukhkar, R. J. Stafford, S. H. Cho, J. W. Tunnell, J. D. Hazle, S. Krishnan, *Nano Lett.* 2008, 8, 1492.
- [229] E. B. Dickerson, E. C. Dreaden, X. Huang, I. H. El-Sayed, H. Chu, S. Pushpanketh, J. F. McDonald, M. A. El-Sayed, *Cancer Lett.* 2008, 269, 57.
- [230] T. Pincus, G. Ferraccioli, T. Sokka, A. Larsen, R. Rau, I. Kushner, F. Wolfe, Rheumatology 2002, 41, 1346.
- [231] G. F. Paciotti, L. Myer, D. Weinreich, D. Goia, N. Pavel, R. E. McLaughlin, L. Tamarkin, *Drug Deliv.* 2004, 11, 169.
- [232] E. E. Connor, J. Mwamuka, A. Gole, C. J. Murphy, M. D. Wyatt, Small 2005, 1, 325.
- [233] S. I. Stoeva, F. Huo, J.-S. Lee, C. A. Mirkin, J. Am. Chem. Soc. 2005, 127, 15362.
- [234] T. A. Larson, J. Bankson, J. Aaron, K. Sokolov, Nanotechnology 2007. 18.
- [235] X. J. Ji, R. P. Shao, A. M. Elliott, R. J. Stafford, E. Esparza-Coss, J. A. Bankson, G. Liang, Z. P. Luo, K. Park, J. T. Markert, C. Li, J. Phys. Chem. C 2007, 111, 6245.
- [236] C. Wang, J. Chen, T. Talavage, J. Irudayaraj, Angew. Chem. Int. Ed. 2009, 48, 2759.
- [237] M. Qu, M. Mehrmohammadi, S. Emelianov, Small 2011, 7, 2858.
- [238] M. P. Melancon, W. Lu, M. Zhong, M. Zhou, G. Liang, A. M. Elliott, J. D. Hazle, J. N. Myers, C. Li, R. J. Stafford, *Biomaterials* 2011, 32, 7600.
- [239] Z. Fan, M. Shelton, A. K. Singh, D. Senapati, S. A. Khan, P. C. Ray, ACS Nano 2012, 2, 1065.
- [240] L. Cheng, K. Yang, Y. Li, X. Zeng, M. Shao, S.-T. Lee, Z. Liu, Biomaterials 2012, 33, 2215.
- [241] L. Cheng, K. Yang, Y. Li, J. Chen, C. Wang, M. Shao, S.-T. Lee, Z. Liu, Angew. Chem. Int. Ed. 2011, 50, 7385.
- [242] R. H. Baughman, A. A. Zakhidov, W. A. d. Heer, Science 2002, 297, 787.
- [243] K. Kostarelos, A. Bianco, M. Prato, Nat. Nanotechnol. 2009, 4, 627.

- [244] N. W. S. Kam, M. O'Connell, J. A. Wisdom, H. J. Dai, Proc. Natl Acad. Sci. USA 2005, 102, 11600.
- [245] G.-P. Wang, E.-Q. Song, H.-Y. Xie, Z.-L. Zhang, Z.-Q. Tian, C. Zuo, D.-W. Pang, D.-C. Wu, Y.-B. Shi, Chem. Commun. 2005, 4276.
- [246] Z. Liu, W. B. Cai, L. N. He, N. Nakayama, K. Chen, X. M. Sun, X. Y. Chen, H. J. Dai, Nat. Nanotechnol. 2007, 2, 47.
- [247] K. Kostarelos, L. Lacerda, G. Pastorin, W. Wu, S. Wieckowski, J. Luangsivilay, S. Godefroy, D. Pantarotto, J. P. Briand, S. Muller, M. Prato, A. Bianco, *Nat. Nanotechnol.* 2007, 2, 108.
- [248] L. Lacerda, A. Soundararajan, R. Singh, G. Pastorin, K. T. Al-Jamal, J. Turton, P. Frederik, M. A. Herrero, S. L. A. Bao, D. Emfietzoglou, S. Mather, W. T. Phillips, M. Prato, A. Bianco, B. Goins, K. Kostarelos, Adv. Mater. 2008, 20, 225.
- [249] C. Zavaleta, A. de la Zerda, Z. Liu, S. Keren, Z. Cheng, M. Schipper, X. Chen, H. Dai, S. S. Gambhir, Nano Lett. 2008, 8, 2800.
- [250] P. Cherukuri, C. J. Gannon, T. K. Leeuw, H. K. Schmidt, R. E. Smalley, S. A. Curley, R. B. Weisman, *Proc. Natl Acad. Sci. USA* 2006, 103, 18882.
- [251] S. Keren, C. Zavaleta, Z. Cheng, A. de la Zerda, O. Gheysens, S. S. Gambhir, Proc. Natl Acad. Sci. USA 2008, 105, 5844.
- [252] K. Welsher, Z. Liu, D. Daranciang, H. Dai, Nano Lett. 2008, 8, 586
- [253] A. De La Zerda, C. Zavaleta, S. Keren, S. Vaithilingam, S. Bodapati, Z. Liu, J. Levi, B. R. Smith, T. J. Ma, O. Oralkan, Z. Cheng, X. Y. Chen, H. J. Dai, B. T. Khuri-Yakub, S. S. Gambhir, *Nat. Nan-otechnol.* 2008, 3, 557.
- [254] N. W. S. Kam, Z. Liu, H. J. Dai, J. Am. Chem. Soc. 2005, 127, 12492.
- [255] N. W. S. Kam, Z. A. Liu, H. J. Dai, Angew. Chem. Int. Ed. 2006, 45, 577.
- [256] Z. Liu, X. M. Sun, N. Nakayama-Ratchford, H. J. Dai, ACS Nano 2007, 1, 50.
- [257] Z. Liu, K. Chen, C. Davis, S. Sherlock, Q. Cao, X. Chen, H. Dai, Cancer Res 2008, 68, 6652.
- [258] H. Ali-Boucetta, K. T. Al-Jamal, D. McCarthy, M. Prato, A. Bianco, K. Kostarelos, Chem. Commun. 2008, 459.
- [259] R. P. Feazell, N. Nakayama-Ratchford, H. Dai, S. J. Lippard, J. Am. Chem. Soc. 2007, 129, 8438.
- [260] S. Dhar, Z. Liu, J. Thomale, H. Dai, S. J. Lippard, J. Am. Chem. Soc. 2008, 130, 11467.
- [261] M. Zhang, T. Murakami, K. Ajima, K. Tsuchida, A. S. D. Sandanayaka, O. Ito, S. Iijima, M. Yudasaka, Proc. Natl Acad. Sci. USA 2008, 105, 14772
- [262] A. Burke, X. Ding, R. Singh, R. A. Kraft, N. Levi-Polyachenko, M. N. Rylander, C. Szot, C. Buchanan, J. Whitney, J. Fisher, H. C. Hatcher, J. Ralph D'Agostino, N. D. Kock, P. M. Ajayan, D. L. Carroll, S. Akman, F. M. Torti, S. V. Torti, *Proc. Natl Acad. Sci. USA* 2009, 106, 12897.
- [263] P. Chakravarty, R. Marches, N. S. Zimmerman, A. D.-E. Swafford, P. Bajaj, I. H. Musselman, P. Pantano, R. K. Draper, E. S. Vitetta, Proc. Natl Acad. Sci. USA 2008, 105, 8697.
- [264] B. Kang, D. Yu, Y. Dai, S. Chang, D. Chen, Y. Ding, Small 2009, 5, 1292.
- [265] R. Singh, D. Pantarotto, L. Lacerda, G. Pastorin, C. Klumpp, M. Prato, A. Bianco, K. Kostarelos, *Proc. Natl Acad. Sci. USA* 2006, 103, 3357.
- [266] M. L. Schipper, N. Nakayama-Ratchford, C. R. Davis, N. W. S. Kam, P. Chu, Z. Liu, X. M. Sun, H. J. Dai, S. S. Gambhir, Nat. Nanotechnol. 2008, 3, 216.
- [267] Z. Liu, C. Davis, W. B. Cai, L. He, X. Y. Chen, H. J. Dai, Proc. Natl Acad. Sci. USA 2008, 105, 1410.
- [268] G. Korneva, H. Ye, Y. Gogotsi, D. Halverson, G. Friedman, J.-C. Bradley, K. G. Kornev, Nano Lett. 2005, 5, 879.
- [269] K. B. Hartman, S. Laus, R. D. Bolskar, R. Muthupillai, L. Helm, E. Toth, A. E. Merbach, L. J. Wilson, Nano Lett. 2008, 8, 415.

Adv. Mater. 2012,



www.MaterialsViews.com

- [270] Y.-J. Lu, K.-C. Wei, C.-C. M. Ma, S.-Y. Yang, J.-P. Chen, Colloids Surf. B: Biointerf. 2012, 89, 1.
- [271] D. Yang, F. Yang, J. Hu, J. Long, C. Wang, D. Fu, Q. Ni, Chem. Commun. 2009, 4447.
- [272] F. Yang, C. Jin, D. Yang, Y. Jiang, J. Li, Y. Di, J. Hu, C. Wang, Q. Ni, D. Fu, Eur. J. Cancer 2011, 47, 1873.
- [273] H. Wu, G. Liu, Y. Zhuang, D. Wu, H. Zhang, H. Yang, H. Hu, S. Yang, Biomaterials 2011, 32, 4867.
- [274] J. Miyawaki, M. Yudasaka, H. Imai, H. Yorimitsu, H. Isobe, E. Nakamura, S. Iijima, Adv. Mater. 2006, 18, 1010.
- [275] J. H. Choi, F. T. Nguyen, P. W. Barone, D. A. Heller, A. E. Moll, D. Patel, S. A. Boppart, M. S. Strano, *Nano Lett.* **2007**, *7*, 861.
- [276] X. Ding, R. Singh, A. Burke, H. Hatcher, J. Olson, R. A. Kraft, M. Schmid, D. Carroll, J. D. Bourland, S. Akman, F. M. Torti, S. V. Torti, *Nanomedicine* 2011, 6, 1341.
- [277] D. L. Shi, Y. Guo, Z. Y. Dong, J. Lian, W. Wang, G. K. Liu, L. M. Wang, R. C. Ewing, Adv. Mater. 2007, 19, 4033.
- [278] A. A. Bhirde, V. Patel, J. Gavard, G. Zhang, A. A. Sousa, A. Masedunskas, R. D. Leapman, R. Weigert, J. S. Gutkind, J. F. Rusling, ACS Nano 2009, 3, 307.
- [279] B. Chen, H. Zhang, C. Zhai, N. Du, C. Sun, J. Xue, D. Yang, H. Huang, B. Zhang, Q. Xie, Y. Wu, J. Mater. Chem. 2010, 20, 9895.
- [280] J. Zhang, J. Ge, M. D. Shultz, E. Chung, G. Singh, C. Shu, P. P. Fatouros, S. C. Henderson, F. D. Corwin, D. B. Geohegan,

- A. A. Puretzky, C. M. Rouleau, K. More, C. Rylander, M. N. Rylander, H. W. Gibson, H. C. Dorn, *Nano Lett.* **2010**, *10*, 2843.
- [281] J.-W. Kim, E. I. Galanzha, E. V. Shashkov, H.-M. Moon, V. P. Zharov, Nat. Nanotechnol. 2009, 4, 688.
- [282] E. I. Galanzha, E. V. Shashkov, T. Kelly, J.-W. Kim, L. Yang, V. P. Zharov, Nat. Nanotechnol. 2009, 4, 855.
- [283] L. Beqa, Z. Fan, A. K. Singh, D. Senapati, P. C. Ray, ACS Appl. Mater. Interfaces 2011, 3, 3316.
- [284] C. R. Martin, Science 1994, 266, 1961.
- [285] D. T. Mitchell, S. B. Lee, L. Trofin, N. Li, T. K. Nevanen, H. Soderlund, C. R. Martin, J. Am. Chem. Soc. 2002, 124, 11864.
- [286] A. Nan, X. Bai, S. J. Son, S. B. Lee, H. Ghandehari, *Nano Lett.* 2008, 8, 2150.
- [287] H. Hillebrenner, F. Buyukserin, M. Kang, M. O. Mota, J. D. Stewart, C. R. Martin, J. Am. Chem. Soc. 2006, 128, 4236.
- [288] S. J. Son, S. B. Lee, J. Am. Chem. Soc. 2006, 128, 15974.
- [289] S. J. Son, J. Reichel, B. He, M. Schuchman, S. B. Lee, J. Am. Chem. Soc. 2005, 127, 7316.
- [290] X. Bai, S. J. Son, S. Zhang, W. Liu, E. K. Jordan, J. A. Frank, T. Venkatesan, S. B. Lee, *Nanomedicine* 2008, 3, 163.
- [291] S. Mitragotri, J. Lahann, Nat. Mater. 2009, 8, 15.
- [292] S. M. Moghimi, A. C. Hunter, J. C. Murray, *Pharmacol. Rev.* 2001, 53, 283.
- [293] R. K. Jain, Annu. Rev. Biomed. Eng. 1999, 1, 241.
- [294] H. Maeda, J. Wu, T. Sawa, Y. Matsumura, K. Hori, J. Controlled Release 2000, 65, 271.